

Geospatial Suitability Assessment of Wetland Soils for Rice Production in Federal University of Agriculture Abeokuta, Ogun State, Nigeria

Anthony Tobore^{1✉}, Oludare Adedeji², Senjobi Bolarinwa¹, Sodiq Olalere²

¹Department of Soil Science and Land Management, College of Plant Science and Crop Production, Federal University of Agriculture Abeokuta, Ogun State, Nigeria. P.M.B. 2240, Abeokuta, Ogun State, Nigeria.

²Department of Environmental Management and Toxicology, College of Environmental Resources management, Federal University of Agriculture Abeokuta, Ogun State, Nigeria. P.M.B. 2240, Abeokuta, Ogun State, Nigeria.

✉Corresponding author:

Anthony Tobore

Phone number: +2348108840248

Email: anthonytobore@gmail.com

Article History

Received: 04 November 2020

Accepted: 16 December 2020

Published: January 2021

Citation

Anthony Tobore, Oludare Adedeji, Senjobi Bolarinwa, Sodiq Olalere. Geospatial Suitability Assessment of Wetland Soils for Rice Production in Federal University of Agriculture Abeokuta, Ogun State, Nigeria. *Discovery Agriculture*, 2021, 7(17), 1-25

Publication License



© The Author(s) 2021. Open Access. This article is licensed under a [Creative Commons Attribution License 4.0 \(CC BY 4.0\)](https://creativecommons.org/licenses/by/4.0/).

General Note



Article is recommended to print as color version in recycled paper. *Save Trees, Save Nature.*

ABSTRACT

Wetland's values are considered an important part of global ecosystems. The primary aim of this study was to develop a methodology for the assessment of wetland suitability potential by employing a Geographic information system (GIS) and Remote sensing (RS) technique. This method applied to the Federal University of Agriculture Abeokuta, Ogun State, Nigeria. Soil samples (0 to 30cm depth) were collected, analyzed, and interpolated using Inverse distance weighted techniques in ArcGIS 10. Supervised

classification algorithm was used to get land cover information using Landsat 8 Operational land images. A GIS-based land suitability analysis was performed after identifying the following criteria: Land surface temperature, Modified normalized difference water index, Land use/land cover, Soil adjusted vegetation index, and Enhanced built-up and bare land index of the study area. The relative importance of each criterion was assessed utilizing the Analytical hierarchy process in Multi-criteria decision making. Land suitability index was calculated and a suitability map was produced. The result of the suitability map shows that 28.9% and 33.2% was moderately and marginally suitable, while 37.9% was marginally not suitable for rice production. The present study demonstrated the efficiency of GIS and RS data for wetland sustainability.

Keywords: Wetland; rice; geographic information system; remote sensing; analytical hierarchy process.

1. INTRODUCTION

Wetlands are areas whose formation is influenced by ecological, hydrological, and geomorphological processes (Frenken and Mharapara, 2002). The desire to find the right balance between the exploitation of wetland services and their conservation has led to an increase in wetland benefits to humans (Mitsch and Gosselink 1993). Wetland degradation may increase in the next 50 years if wetlands ecosystem services and functions are not effectively managed and monitored (MA, 2005b). Moreover, due to the increasing world population and the growing pressure on food production, sub-Saharan Africa such as Nigeriamay experience food scarcity by the year 2020 (Joshua et al. 2013). In recent decades, the use of wetlands has increased significantly in many developing countries (McCartney et al. 2010). In Nigeria, wetland areas cover 7.2 percent of the total land area of the country (Ojanuga, 2006). However, the occurrence of wetland soils in Nigeria has been associated more with rice production with three landforms namely; inland depressions, floodplains, and coastal plains (Fasina, 2005).

Rice (*Oryzasativa*) belongs to the Gramineae family and constitutes a significant component of major staple food crops (Ayolagha et al. 2012). Suitability of wetland soils for optimum rice production depends on the underlying parent material, topography, land use, temperature, and rainfall,etc. (Ahukaemere and Akpan, 2012). However, many wetland soils around the world are becoming more unsustainable. Hence, calls for geospatial techniques that serve as a bottom-up approach for consistent mapping at national, regional, and local levels (Karimi and Zeinivand, 2019). Land suitability analysis is a geographic information system (GIS) based application used in sustainably determining crop suitability (Zubair, 2006; Mustafa, 2011; Saaty, 1977; Jafari and Zaredar 2010; Vargahan et al. 2011). On the other hand, Remote Sensing (RS) techniques serve as valuable tools for the assessment of the well-being of wetlands at different scales (Merollaet al.1994; Davis, 2009). In the last few decades, integration of RS and GIS using the Analytical hierarchy process (AHP) has been widely applied to land suitability assessment problems (Kahinda et al. 2008; Mahmoud and Alazba 2014; Thapa and Murayama 2008; Cengiz and Akbulak 2009; Patil et al. 2012. The AHP serves as a powerful pair-wise comparison matrix that supports spatial decision system on the judgments of expert's priority scales (Thapa and Murayama 2007).

In the present study, remote sensing data and a GIS-based conceptual framework is applied with the Multi-criteria decision-making (MCDM) technique using AHP. The conceptual framework will help to identify the potential suitability of the wetland soils for rice production at the Federal University of Agriculture Abeokuta, Ogun State, Nigeria using geospatial techniques.

Study Area

The methodology of the land suitability evaluation was applied to the Federal University of Agriculture Abeokuta (FUNAAB) located next to the Ogun-Osun River Basin Development Authority (OORBDA) in the Northern part of Abeokuta city, Ogun state, Nigeria. The area is geographically described by latitudes 7° 13'N and 7° 20'N and by longitudes 3° 20'E and 3° 28'E enclosing approximately 10,000 hectares (ha) of land area (Figure 1). It is characterized by undulating with extensively mild slopes bounded into six zones and punctuated in parts by ridges, isolated residual hills, plateaus, and valley landscapes with low lands (Savage, 2010). The area is mainly drained by the Ogun River and other streams namely: Oshinko, Ole, Alakata, Arakanga, Pala, Olu, Tigba, and Ajigbayin (Ufoegbune et al. 2010).

Geology and soil

The geology of the study area overlies metamorphic rocks of the basement complex, the majority of which are ancient being of pre-Cambrian age with great variation in grain size and mineral composition. This rock ranges from very coarse grain pegmatite to fine-grained schist and from acid quartzite to basic rocks consisting largely of amphibolites (Smyth and Montgomery, 1962). The area is sub-divided into sedentary, hill-creep, and hill-wash soils with the development of lowland forests (FAO/IUSS 2006; Ekanade, 2007).

The soils of the study area are dry for as long as 90 days and thus considered as the Udic moisture regime and therefore classified as Isohyperthermic temperature (Soil Survey Staff, 2010). For easy and efficient mapping of the study area, the soil classification map (Figure 2) produced by Sotona et al. (2013) was further modified and used for this study.

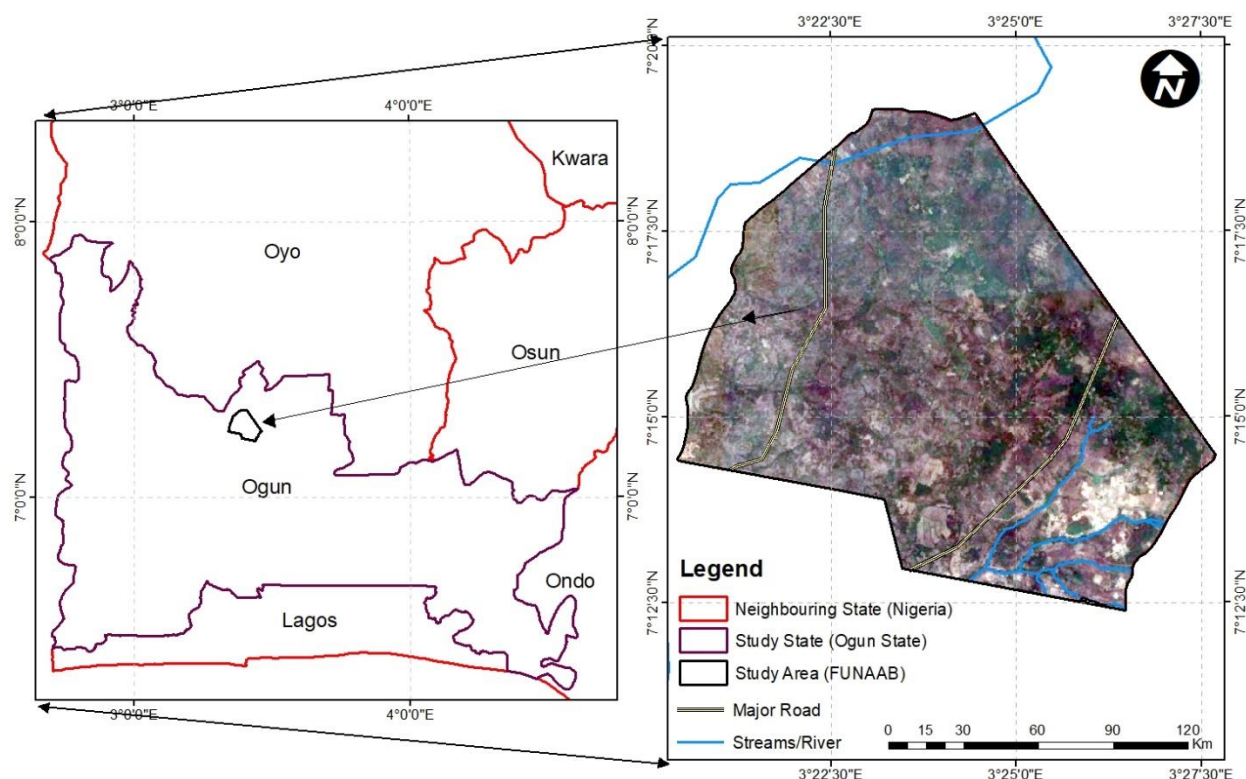


Figure 1: Study area

Climate

The climate of the study area is humid tropical type having an annual rainfall of about 2500 mm (at the coast) to 1220 mm (at the northern limit) which runs from April to October and characterized by a wet and dry season (Adebekun, 1978). The minimum and maximum temperature is about 22.48°C to 31.24°C with an average yearly temperature of about 26.6°C.

2. METHODOLOGY

In this study, land suitability analysis was integrated with RS and GIS in MCDA to determine the suitability of the study soil for rice production. The present study employed the following steps in achieving the methodology:

1. Identification and development of a GIS database using multi-criteria suitability requirements.
2. Processing and creation of RS and GIS data to compile criteria maps for suitability analysis.
3. Determination of suitability level and scoring scale based on suitability criteria evaluation.
4. Application of AHP for the assessment of the relative importance of each criteria weights.
5. Application of a weighted overlay method for estimation of the land suitability index (LSI).
6. Evaluation and reclassification of land suitability criteria into land suitability classes.
7. Identifying areas with most suitable for rice cultivation.

Rainfall Analysis

The present study utilized the annual rainfall and Standardized precipitation index (SPI) approach for rainfall variability assessment of the study area. A total of 10 years (2009 to 2018) rainfall data were collected at the Department of Agro-meteorology and Water Management, College of Environmental Resources Management, FUNAAB. The SPI and annual rainfall data collected were used to assess the wetland potential of the study area for rice production. Table (1) shows the SPI classification for any location-based using

precipitation records (Doesken, and Kleist 1993). The SPI described by Akinsanola and Ogunjobi (2014) and Adegoke and Sojobi (2015) was used in this study and expressed as:

$$SPI = \frac{X - \bar{X}}{\sigma} \dots \dots \dots \text{Equation 1}$$

Where X: The rainfall in each particular year, \bar{X} : The mean rainfall in each particular year, σ : The standard deviation of rainfall in each particular year.

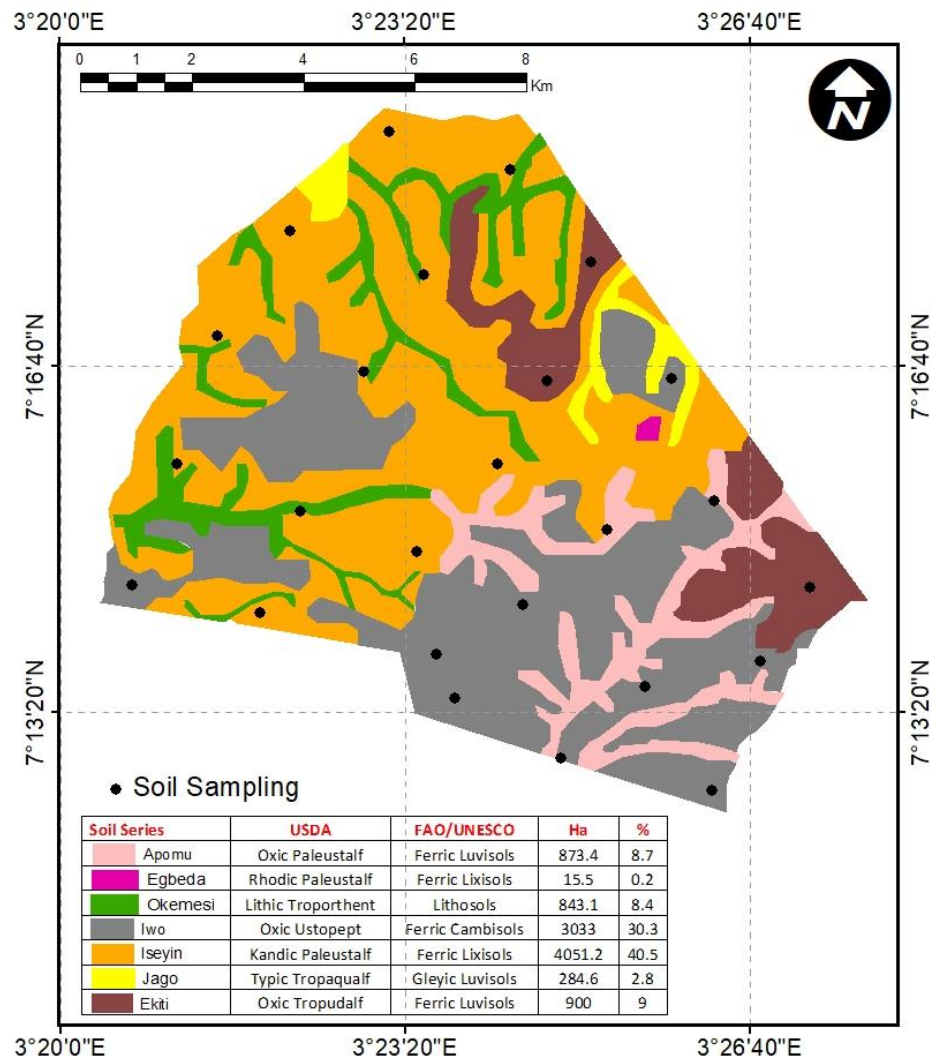


Figure 2: Soil classification of the study area

Table 1: Annual standardized precipitation index given by McKee, Doesken, and Kleist (1993).

Classification	SPI
Near Normal	-0.99 to 0.99
Moderately wet years	1.0 – 1.49
Moderately dry years	-1.0 to -1.49
Very wet	1.5 to 1.99
Severely dry years	-1.5 to -1.99
Wet extreme	≥ +2.0
Dry extreme	≤ - 2.0

Processing and creation of spatial data layers

Modified Normalized Difference Water Index

Remote sensing data provide spectral indices for extracting information from Earth's surface such as waterbodies, soil, and surface temperature, etc. (Yang, *et al.*, 2003). The present study employed the use of a Modified normalized difference water index (MNDWI) to effectively assess the presence of waterbodies in the study area. The MNDWI was used to remove or suppress the vegetation and soil noise effects from the study area (Xu, 2005). To perform the MNDWI, Landsat 8 Operational land images (OLI) and Thermal infrared sensor (TIRS) of the year 2015 and 2020 was acquired and downloaded from the United States Geological Survey (USGS) website repository. The acquired Landsat 8 OLI was further subjected to simplified data processing and user image interpretation in ArcGIS 10 ESRI (Environmental Systems Research Institute). Thereafter, a raster math calculator in spatial analyst tools was used to perform the MNDWI operation in the study area using the equation described by Xu, (2005):

$$MNDWI = \frac{(Green - MIR)}{(Green + MIR)} \dots \dots \dots Equation 1$$

Where: Green represents band 3, and MIR (Middle Infrared) represents and 6 of the Landsat 8 OLI dataset.

Enhanced Built-up and Bareness Index

Application of Enhanced built-up and bareness index (EBBI) depends on the types of the satellite image, accuracy level, surface characteristics, and the purpose of the study (As-syakur *et al.* 2012). Study conducted by Li *et al.* (2017) revealed that EBBI serves as an efficient approach used in extracting built-up area and bareland cover information. Therefore, in this study, the EBBI was used to extracts information on the built-up and bare land using Landsat 8 dataset of the years 2015 and 2020. The EBBI of the study area was derived using the equation described by As-syakur *et al.* (2012):

$$EBBI = \frac{(SWIR - NIR)}{(10 * \text{root} (SWIR + TIR))} \dots \dots \dots Equation 2$$

Where; SWIR represents Short-wavelength infrared of band 6 in Landsat 8 OLI, NIR represents the Near-infrared of band 5 in Landsat 8 OLI and TIR represents Thermal infrared of band 10 in Landsat 8 OLI.

Vegetation cover analysis

Vegetation indices are one of the primary sources of information used in monitoring the Earth's vegetation cover (Gilabert *et al.* 2002). The present study, utilized the Soil adjusted vegetation index (SAVI) to assess the vegetation cover of the study area using Landsat 8 datasets of the years 2015 and 2020. The SAVI was used due to its ability to correct the soil brightness in a study especially when the vegetation cover is low (Jiang *et al.* 2006). The SAVI described by Huete, (1988) and Verbesselt *et al.* (2006b) was used in this study and derived using the following equation:

$$SAVI = \frac{(NIR - Red)}{(NIR + Red + L)(1 + L)} \dots \dots \dots Equation 3$$

Where: NIR is the Near-infrared regions of band 5, Red is the visible red of band 4 and L is the constant or correction factor, ranges from 0 to 1.

Land surface temperature

Accurate Land surface temperature (LST) retrieval from remote sensing data depends on emissivity and geometry (Gao *et al.* 2013). For this study, LST was calculated using temporal information from the Landsat 8 OLI satellite images of the years 2015 and 2020. The LST of the study area was subjected to two procedures.

Step 1: The SAVI data derived from equation (3) were used to calculate the Proportion of vegetation (PV) of the study area which can be expressed as follows:

$$PV = \left(\frac{SAVI - SAVI_{\min}}{SAVI_{\max} - SAVI_{\min}} \right)^n \dots \dots \dots \text{Equation 4}$$

Where: $SAVI_{\min}$ was retrieved from the SAVI minimum value, which is -1, and $SAVI_{\max}$, retrieved from the SAVI maximum value, which is 1. Therefore, the PV of the study area was further expressed as follows: $PV = \left(\frac{SAVI+1}{2} \right) \dots \dots \dots \text{Equation 5}$

Step 2: The thermal bands were converted to Digital numbers (DNs) to estimate the spectral radiance of the study area using bands 10 and 11 in the Landsat 8 OLI image (Rasul et al.2015). The spectral radiance of the bands was described below and subjected to equation (6):

$$L\lambda = (0.0003342 * \text{Band10} + 0.1 \text{ and } L\lambda = 0.0003342 * \text{Band11} + 0.1) \dots \dots \text{Equation 6}$$

$$L\lambda = ML + Q_{CAL} + AL$$

Where: $L\lambda$ is the TOA (Top of atmosphere) spectral radiance at the sensors aperture

ML is the band-specific multiplicative rescaling factor from the metadata,

Q_{CAL} is the quantized and calibrated standard product of the digital pixel values,

AL is the band-specific additive rescaling factor from the metadata.

Thereafter, Land surface emissivity (LSE) and Brightness temperature (BT) of the study area was calculated and described using equations (7) and (8). Hence, the LST of the study area was further calculated using equation (9) and expressed according to Jesus and Santana (2017):

$$LSE = 0.004 * PV + 0.986 \dots \dots \dots \text{Equation 7}$$

$$BT = \frac{K2}{\ln \left\{ \frac{K1}{L\lambda} \right\} + 1} - 273.15 \dots \dots \dots \text{Equation 8}$$

Where: BT is the satellite brightness temperature (Celsius)

K2 is the calibration constant 2 (Kelvin), thermal conversion constant from the metadata;

K1 is the calibration constant 1 (Kelvin), thermal conversion constant from the metadata;

$$LST = \frac{BT}{1 - \left(\frac{\lambda_{BT}}{PV} * \ln LSE \right)} \dots \dots \dots \text{Equation 9}$$

Principal component analysis

Principal components analysis (PCA) is a set of multivariate statistics that correlate variables and transform them into uncorrelated variables in the satellite image bands (Weng, 2012). The present study employed the use of PCA to improve the quality of the land use/land cover (LULC) classification of the study area (Singh and Harrison, 1985). To perform the PCA of the study area, Landsat 8 OLI satellite of the year 2015 and 2020 images were used in the ENVI software environment. The Landsat 8 satellite images were further subjected to data processing such as data redundancy, pre-processing, geometric adjustment, and conversion of DN to reflectance values using Dark object subtraction (DOS) in ENVI software⁵¹⁻⁵² (Chavez, 1998; Chuvieco, 2002; Weng, 2012). The essence of this operation is to enhance the visual interpretation of the Landsat images for better enhancement during the analysis of the LULC change of the study area. The characteristics of the downloaded Landsat satellite images used for this study were shown in Table (2). The PCA of the study area was calculated and expressed according to Estornell et al. (2013) using equation (10). To calculate the eigenvector from the vector-matrix, an equation derived from Estornell et al. (2013) in equation (11) was used:

$$Y^8 = \begin{pmatrix} y^1 \\ y^2 \\ \vdots \\ y_b \end{pmatrix} = \begin{pmatrix} w^{1,1} & \dots & w^{1,b} \\ \vdots & \ddots & \vdots \\ w^{b,1} & \dots & w^{b,b} \end{pmatrix} \begin{pmatrix} x^1 \\ x^2 \\ \vdots \\ x_b \end{pmatrix} \dots \dots \dots \text{Equation 10}$$

Where: Y is the vector of the principal components, w: is the coefficient of the transformation matrix of the eigenvectors in the diagonal covariance matrix of the original bands, and x: is the vector of the original data.

$$(C - \lambda_k I)W_k = 0 \dots \dots \dots \text{Equation 11}$$

Where: C is the covariance matrix, λ_k is the k eigenvalues (Eleven in a Landsat OLI image composition), I: is the diagonal identity matrix, and W_k is the K eigenvectors.

Table 2: Characteristics of Landsat 8 OLI images used in the study

Metadata	2015	2020
Acquisition date	2015 – 10 - 12	2020 – 10 - 20
Scene center time	10:03:03	10:03:05
Path	191	191
Row	055	055
Sensor and platform	OLI-TIRS	OLI-TIRS
Processing level	Calibration	Calibration
Number of bands	11	11
Sun azimuth	142.77069460	134.88500186
Sun Elevation	52.10216187	50.77679746

Land use/Land cover Analysis

The acquired satellite images were enhanced in the Idrisi selva Software environment via (3 by 3) majority filter techniques for better visibility during analysis. True colour composite (TCC) was generated using suitable combinations of bands in the PCA images (d'Entremont and Thomason, 1987; Good and Giordano, 2019). Considering the "Nigeria land use classification System" and the goal of this study, Anderson et al. (1976) land use classification scheme II and prior knowledge of the study area for over 6years was used to identify the Area of interest (AOI) features of the study area. For this study, an unsupervised and supervised classification algorithm was performed in the Idrisi selva environment to assess the nature of change in the study area using Landsat 8 OLI of the year 2015 and 2020 images. Among the supervised classification methods, the maximum likelihood algorithm is one of the most applied methodologies used in monitoring LULC changes especially in the field of agriculture (Biro et al. 2013; Zhang et al. 2015). Besides, maximum likelihood algorithm was considered due to its final outcome result and geovisualization (Silva and Costa, 2015; Liu, 2005; Sun et al. 2013). Therefore, this study employed the maximum likelihood classification system (MLCS) and the unsupervised K- means algorithm to assess the LULC change of the study area. The K- means of unsupervised classification were supported with MLCS due to the heterogeneous nature of wetlands (Harvey and Hill, 2001). The present study classified the LULC into 5 classes based on the MLSC algorithm techniques using the Landsat 8 OLI of the year 2020 (Table 3). The K- means algorithms of unsupervised classification were used to assess the Landsat 8 image of the year 2015. However, due to the complex nature of wetlands, such as seasonal variations and distinct landcover types, Google Earth's image was downloaded from the Google Earth engine repository website to validate the identified AOI of the study area. Thereafter, the classified LULC images of the study area were further subjected to post-classification processing. The essence of this operation was used to remove the misclassified pixels in the outlying LULC images in the study area. Shuttle radar topographic mapper (SRTM) of a 30-meter resolution was used to produced the Digital elevation model (DEM), aspect, stream order, and slope map of the study. The river and road map was also produced and used in the efficient mapping of the study area using ArcGIS 10 ESRI (Fig. 3a, 3b, and 3c).

Table 3: Description of land use and land cover categories

No	Class name	Description
1	Built-up	Lecture hall, offices, and laboratories
2	Vegetation	Mixed forest and grass
3	Bareground	Vacant land, open space, sand, bare soils, and landfill site
4	Farmland	Fallow land rainfed cropping planted cropping areas
5	Wetlands	Waterbodies, river, lakes, ponds creeks, and streams

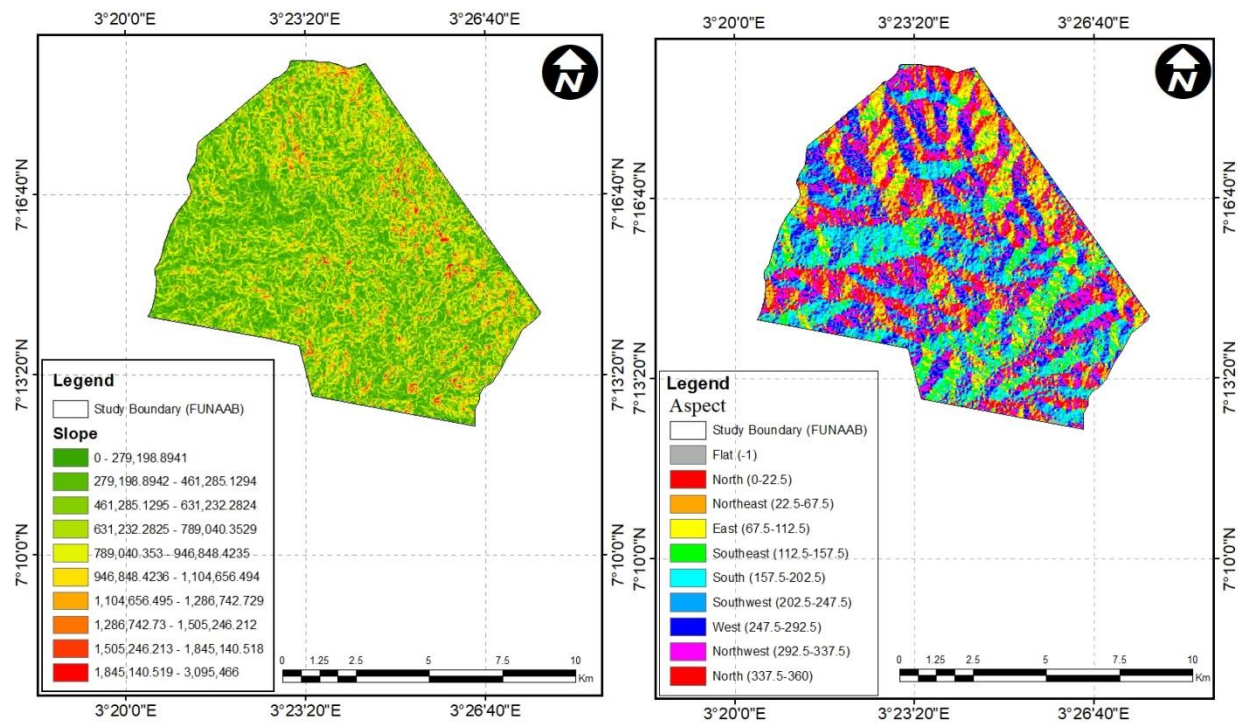


Figure 3a: Slope and Aspect of the study area

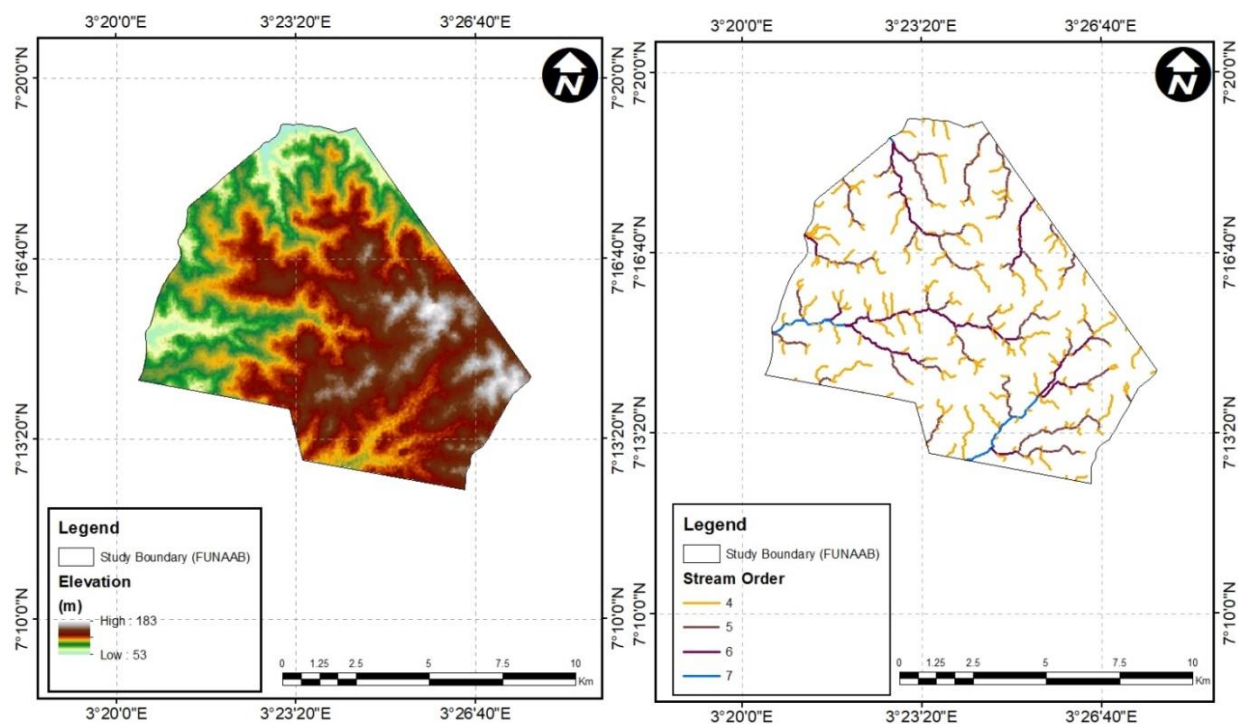


Figure 3b: Slope and Aspect of the study area

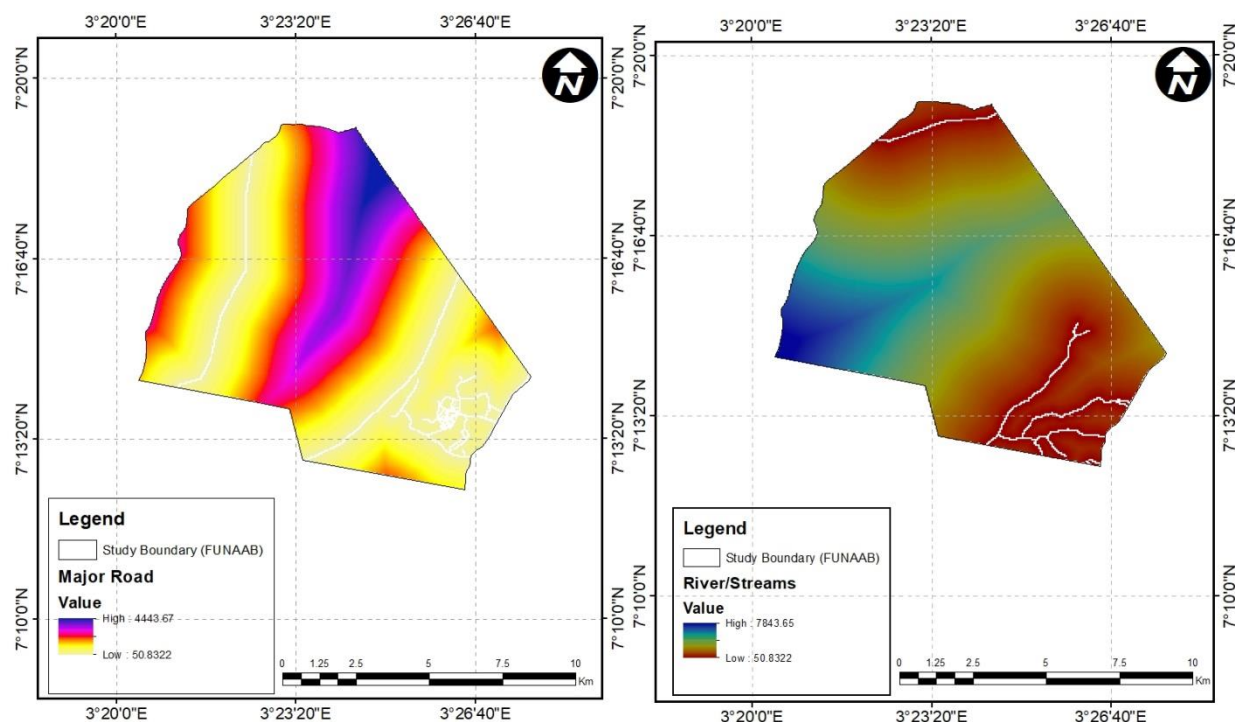


Figure 3c: Slope and Aspect of the study area

Precision Accuracy Assessment

Precision accuracy assessment of the study area was carried out by comparing the extent of the LULC classes in the classified image to the reference data-set using the classified map (Congalton, 1991). The accuracy of the LULC map of the study area was computed through the following error matrix: Overall accuracy, kappa coefficient, producer's and user's accuracies (Foody, 2002). The overall accuracy is given by the ratio of the proportion of the correctly classified pixels to the total number of pixels in the error matrix ⁶⁴ (Pontius Jr and Millones, 2011). To compute the error matrix in this study, the following formula was used.

$$\text{Producer accuracy} = \frac{\text{Area properly identified in a classification method}}{\text{The area in the reference ground truth}} \dots \text{Equation 12}$$

$$\text{User accuracy} = \frac{\text{Area properly identified in a classification method}}{\text{Total area calculated from the method}} \dots \dots \dots \text{Equation 13}$$

$$\text{Kappa coefficient} = \frac{\text{Observed accuracy} - \text{Expected agreement}}{1 - \text{Expected agreement}} \dots \dots \dots \text{Equation 14}$$

Soil Mapping and Analysis

Reconnaissance and stratified random sampling were employed based on the soil survey manual (FAO, 2007a). A hard copy of the study area soil map was downloaded in the Geographic tagged image file (GeoTiff), scanned, and georeferenced in ArcGIS 10 ESRI (See figure 2). Coordinates of the study area soil types were retrieved from the scanned georeferenced soil map and further stored using a handheld Global positioning system (GPS) device. This operation was performed to allow accurate mapping and identification of the soil types in the study area. Thereafter, 5 representative soil samples were collected using a soil auger from each soil type at a predetermined interval making a total of 35 soil samples. The representative's soil samples were collected at the soil depth of 0 – 30cm for soil analysis. The soil samples collected were processed in the laboratory after air-drying at room temperature for soil analysis. The entire soil auger observations were stored and inputted with the help of handheld GPS for spatial mapping of the study area. Other physiographic features coordinate points were taken with the aid of a GPS and properly documented to assist in the adequate mapping of the study area.

Laboratory Data Analysis

The following soil parameters were determined: nitrogen, potassium, phosphorus, hydrogen ions, soil texture, and soil pH. The particle size was determined by hydrometer method Bouyoucos described in Beretta et al., (2014). Total nitrogen was determined calorimetrically. Available phosphorus was extracted by Bray 1 method (Anderson and Ingram, 1993; Flavio et al., 2011) and phosphorus concentration was determined using a ultra violet spectrophotometer. Soil organic carbon was determined by dichromate oxidation procedure and organic matter was determined by 1.724 of carbon factor. Exchangeable bases (Calcium, Magnesium, Potassium, and Sodium) were extracted with neutral ammonium acetate. Ca and Mg were determined with Atomic Absorption spectrometry while K and Na were determined by flame photometer. Base saturation and effective cation exchange capacity were calculated. Soil pH was determined in a 1:2 soil to water suspension using a glass electrode pH meter. Heavy metal analyses, sub-samples (0.5 g) of each of the soil were digested. Digestion was done with 10 ml of a mixture of nitric (HNO₃) and perchloric (HClO₄) acid in ratio 2:1 (v/v) for 90 min, initially at 150° C. After which 2ml of concentrated Hydrochloric Acid (HCL) was added to the mixture. The temperature of the digest was then increased to 230° C for another 30 minutes on the digester. On completion of digestion, digests were allowed to cool down at room temperature. Thereafter, the content of each digestion tube was transferred into a 50 ml volumetric flask and made to volume with distilled.

Data analysis

Descriptive statistics and geostatistics were used to analyze and interpret the soil datasets and spectral index. Descriptive statistics were run in the R package and the pairwise Pearson's correlation between the spectral indices was calculated in RStudio v4.0.3. Thereafter, a correlation plot was generated using the R package "corrplot." Coordinates of the analyzed soil data were saved in excel spreadsheets as text delimited and each of these soil data concentrations was plotted and display in the ArcGIS 10ESRI. The spatial distribution of collected soil nutrients was prepared using Inverse distance weighted (IDW) techniques for soil data interpolation in ArcMap (Li and Heap 2008). IDW is a technique that relies on the significance of known points from the output point (Watson and Philip 1985). Therefore, in this study, the equation (15) derived by Agris (1998) was used to interpolate the estimated values and the weight of the collected soils sample was established using equation (16):

$$Z * (x_0) = \sum_{i=1}^n w_i Z(x_i) \dots \dots \dots \text{Equation 15.}$$

Where: w_i , the weight assigned to the value at each location: $Z(x_i)$ and n , number of close neighboring sample data points used for estimation. Thereafter, a skewness value of < 1 was employed using the IDW (Agris 1998).

$$w_i = \frac{1/dp_i}{\sum_{i=1}^n 1/dp_i} \dots \dots \dots \text{Equation 16.}$$

Where: d_p denotes the distance between point i and the unknown point; p . exponent parameter.

Determining criteria weights using AHP

AHP is a method that combines two or more criteria at a time through a pairwise comparison matrix and consistency ratio (Saaty, 1987). The AHP relies on the relative importance of weight given to one criterion over another (Saaty 1980). The present study utilized the spectral indices (LST, MNDWI, EBBI, SAVI), classified LULC, and the interpolated soil data to determine the relative importance weight of each criterion. The relative preference of the criteria was subjected to a pairwise comparison scale (Table 4). MCDM was used to produce the criteria maps using the calculated weights for each criterion as attribute data. The pairwise comparison matrix approach and consistency ratio (CR) was computed as:

$$CR = \frac{(\lambda_{max} - n)}{RI} \dots \dots \dots \text{Equation 17}$$

Where λ_{max} : is the principal eigen value, n : is the number of elements compared, and RI : is the random consistency index value that depends on the number of criteria that are being compared. The overlay weighted method in spatial analyst tool of ArcGIS 10ESRI was used to estimate the LSI of the study area according to the formula described by Saaty, (1987):

$$V_i = \sum_{j=1}^n w_j \cdot v_{ij} \dots \dots \dots \text{Equation 18}$$

Where V_i is the suitability index in each raster cell, w_j is the weight of criterion, j and n is the total number of criteria. The raster layer of the resulted map was further classified into the adopted FAO (1976) following the procedure described by Sys et al. (1991) land suitability evaluation (Table 5). Thereafter, the classified land suitability map was overlaid with the soil map of the study area.

Table 4: Scale for pairwise comparisons (Saaty 1980)

Intensity of Importance	Definition
1	Equal importance
2	Equal to moderate importance
3	Moderate importance
4	Moderate to strong importance
5	Strong importance
6	Strong to very strong importance
7	Very strong importance
8	Very to the extreme importance
9	Extreme importance

Table 5: Land suitability class description and the corresponding suitability index

Class	Suitability	Suitability Index	Description
S1	Optimally suitable	> 75	Land without any significant limitation
S2	Moderately suitable	50 - 75	A moderately severe limitation which reduces productivity
S3	Marginally suitable	25 - 50	Overall severe limitations; given land use is only marginally justifiable
N1	Marginally not suitable	10 - 25	The land-use type under analysis is not acceptable at all for the land
N2	Permanent Unsuitable	< 10	The land-use type under analysis is permanently not acceptable at all for the land

3. RESULTS AND DISCUSSION

Rainfall Analysis

Table 6: Classification of annual rainfall based on SPI

Classification	Years
Dry extreme Years	
Moderately dry years	
Moderately wet years	2009, 2013, 2017, 2015, 2018.
Near normal years	
Very wet years	2010, 2011, 2012, 2014, 2016.
Wet extreme years	

Rainfall data analysis and SPI calculation were used to assess the dry and wet years of the study area. Classification of the annual rainfall was based on the SPI of the study area. The result showed that the SPI of the studied area falls into moderately wet and very wet years (Table 6). The present result suggests that the precipitation of the studied area can supports wetland potential for optimum rice production.

Analyses of LST, MNDWI, EBBI and SAVI of the study area

Assessment of wetlands potential using spectral satellite image data is widely used due to its ability to provides higher accuracy and tends to be less time-consuming ⁷⁸ (Jensen, 1996). In this study, spatial variation of extracted spectral indices of LST, MNDWI, EBBI, and SAVI has been studied for a period of 5 years from 2015 to 2020 (Figures, 4 to 7). The spatial variation of the LST for both years elaborates that in the year 2015, minimum and maximum temperature experienced in the studied area ranged from 23.4° K to 29.5° K (Celsius). For the year 2020, the maximum temperature tends to decrease from 29.5° K to 25.1° K and the minimum temperature remains 23.4° K in the studied area (Figure 4).According to Sys et al. (1993), LST that ranges from 23.4° K to 25.1° K can be considered favorable for optimum rice production. Also, Liu et al. (2016) and Wang et al. (2018) posits that area or region with low or higher LST is one of the crucial environmental problems faced in the field of agriculture especially wetland soils. As seen in Figures 5, 6, and 7, it can therefore be inferred from the resulted images that MNDWI depicts higher waterbodies coverage in the year 2020 than 2015. McFeeters, (1996) and Chowdary et al. (2010) noted that MNDWI serves as one of the well-established means of detecting surface waterbodies due to higher reflectance in the SWIR compared with the NIR wavelength range. Similarly, the EBBI in the present study was quite high in the year 2020 indicating the percentage of the built-up and bare land area increased more than EBBI in the year 2015. Therefore, the EBBI used in this study reveals a better accuracy to the built-up areas with a higher degree of correlation in assessing LULC change. The research conducted by Sinha et al. (2016) and Bouhennache et al. (2015) also corroborated with the present study. Besides, the increased experience in both EBBI and MNDWI in the year 2020 could also be traced to anthropogenic activities such as reduction or loss of vegetation cover, etc. Considering the result of the SAVI, it shows that the study area demonstrates very low vegetation densities in the year 2020 than in 2015. The decrease in the year 2020 SAVI could also be responsible for an increase in the EBBI in the year 2020 of the study area. Moreover, Aman et al. (1992) opined that loss or low vegetation directly increases human activities, especially in developing countries such as Nigeria. The MNDWI, EBBI, LST, and SAVI used in this study serves as indispensable spectral indices to assess the rate of change in the study area (Yang, *et al.*, 2003). Tables (7) shows the descriptive statistics of the spectral index of the study area. The statistical data result of the LST, MNDWI, EBBI, and SAVI was assessed and recorded from each indices equation.

Table 7: The statistics summary of each index used in the study area

Statistic	MNDWI		EBBI		SAVI		LST	
	2020	2015	2020	2015	2020	2015	2020	2015
Mean	- 0.05	- 0.20	- 0.31	- 0.22	0.45	0.36	26.40	29.66
Std.dev	0.48	0.20	0.88	0.82	0.25	0.15	1.76	2.97
Min.	- 0.61	- 0.72	- 1.88	- 1.38	0.03	0.05	23.43	25.13
Max	1.20	0.09	1.32	1.25	1.01	0.57	29.50	35.42

Min: Minimum; Max: Maximum; Std.dev: Standard deviation.

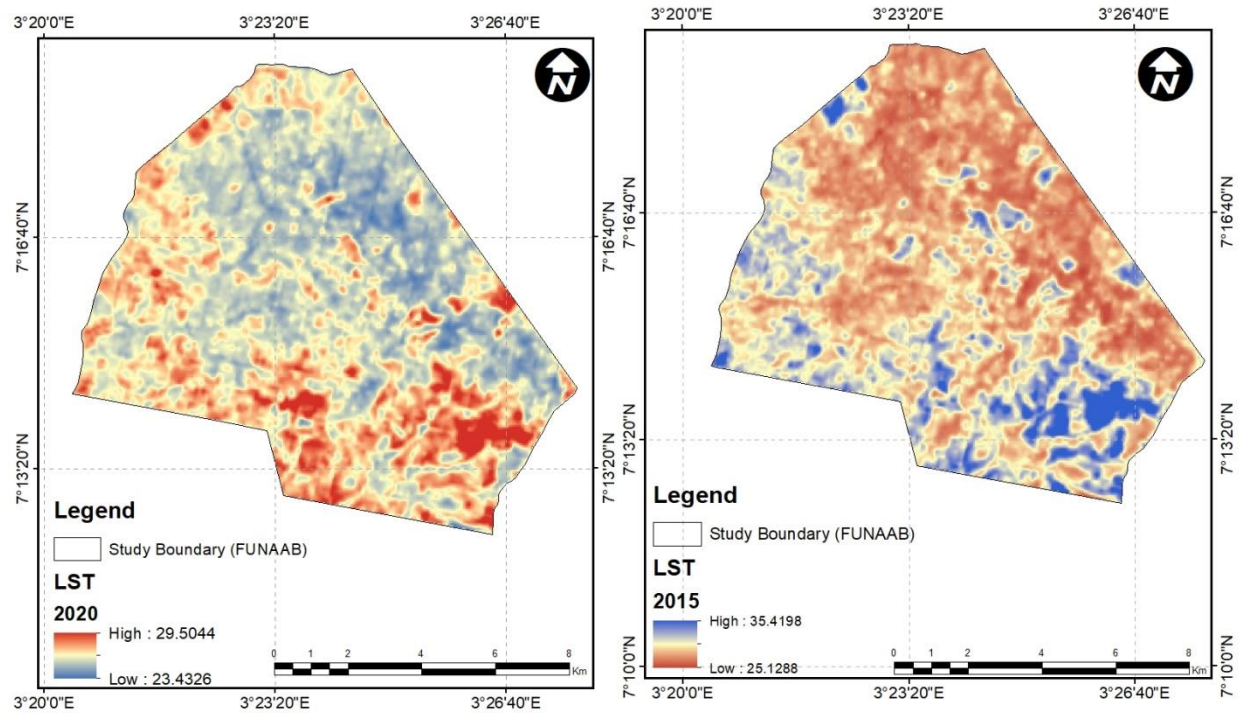


Figure 4: Land surface Temperature of the study area

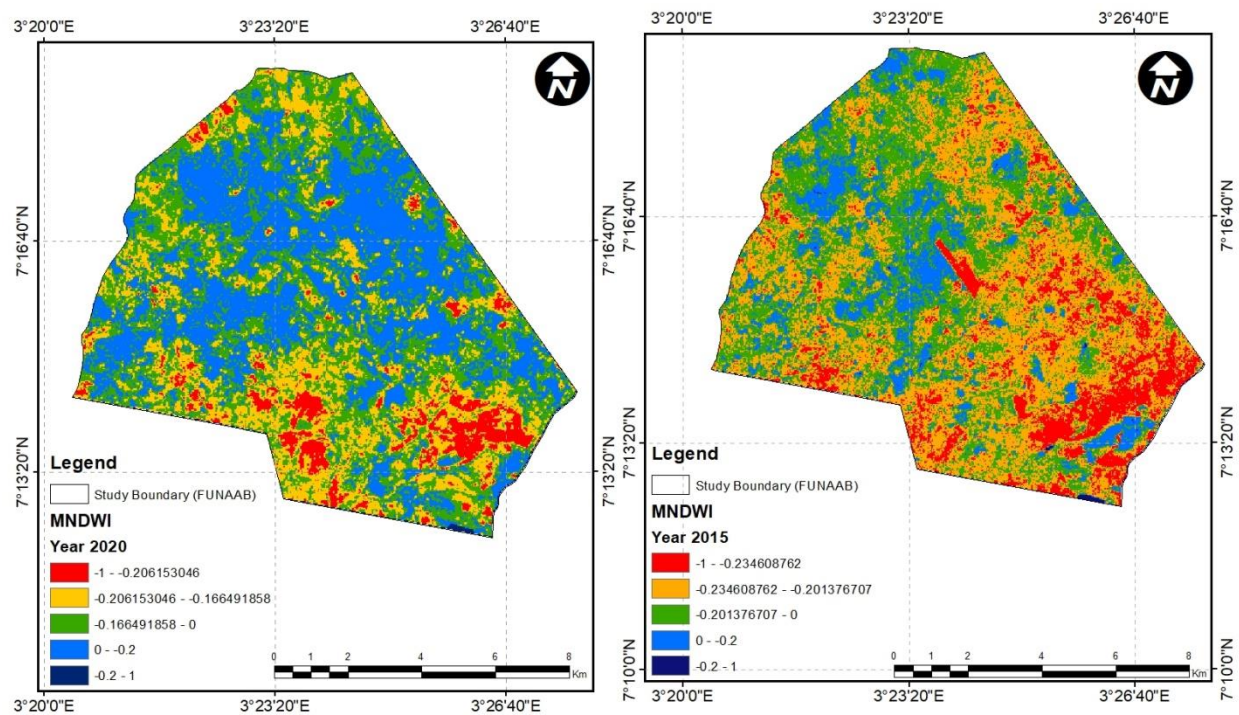


Figure 5: Modified Normalized Difference Water Index of the study area

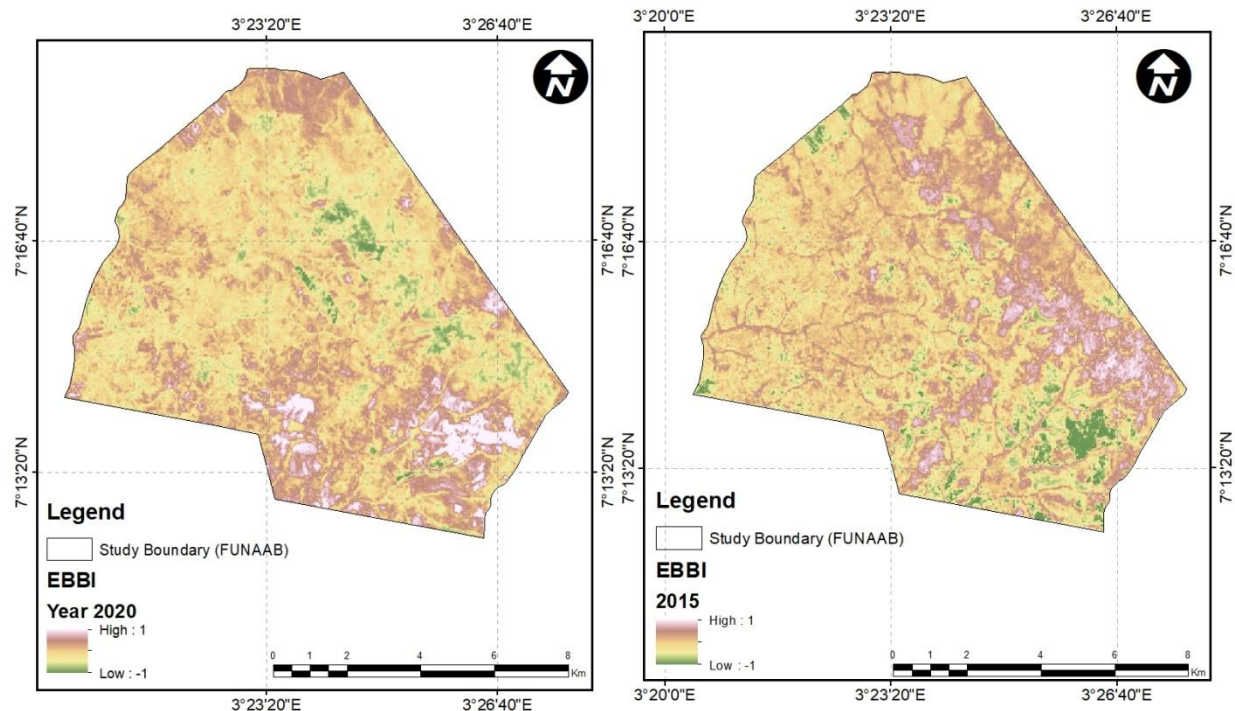


Figure 6: Enhanced Builtup and Bareness Index of the study area

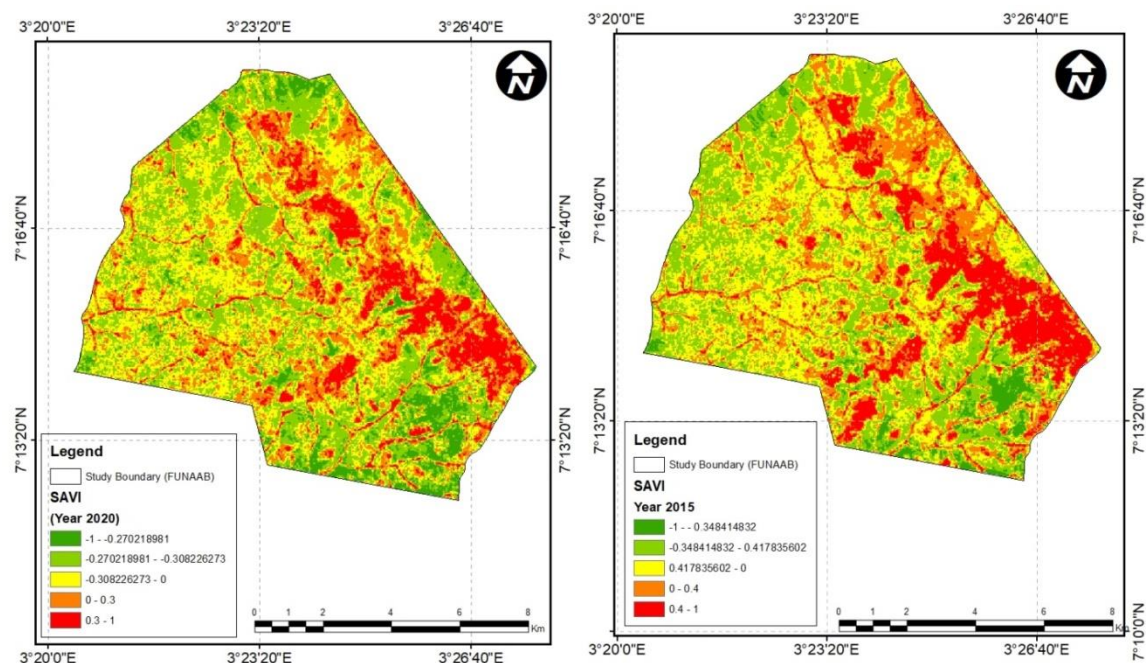


Figure 7: Soil Adjusted Vegetation Index of the study area

Correlation between spectral indices

The spectral index of LST with MNDWI ($r^2 = 0.80$, $P < 0.02$), and LST with SAVI ($r^2 = 0.73$, $P < 0.04$), had a strong correlation while LST with EBBI ($r^2 = 0.58$, $P < 0.08$) had a moderate correlation. In general, a strong association between the spectral indices was observed (Figure 8).

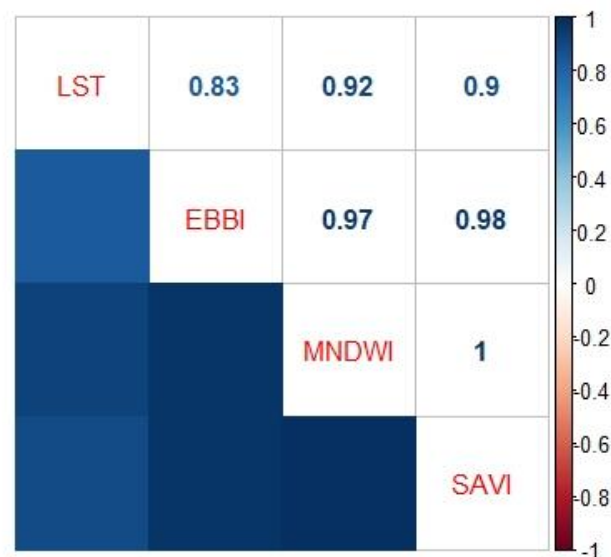


Figure 8: Correlation matrix of the study area.

Principal Component Analysis

The present study employed the principal component techniques to improve the quality of the LULC classification of the study area. In this study, the PCA was applied to the seven bands in the satellite images resulting in the eigenvalues; mean; standard deviation; minimum, and maximum (Tables 8 and 9). The seven bands of satellite images used in this study were employed to remove data redundancy and also to save computation space and time during analysis. As seen in Tables 10 and 11, the PC1, PC2, and PC3 in the year 2015 were negatively loaded on the bands 5 and 6 in the following order: -0.481, -0.476, -0.381, -0.378, and -0.257. It was also observed that PC3, PC4, PC6, and PC7 shows a high positive loading on band 1 (0.623), band 5 (0.683), band 6 (0.813), and band 7 (0.680). In contrast, the PCA of the year 2020 had a negative loading in almost all the image bands. For the positive loading, PC4, PC5, and PC6 show a higher positive loading in band 3 (0.703), band 2 (0.963), and band 4 (0.560). The result of the PCA in this study denotes that satellite bands that are positively loaded mainly represent no change in the overall brightness. The negatively loaded measure the changes in brightness of the two images used in the present study (Koutsias et al. 2009). Also, the application of PCA in this study serves as one of the important pre-processing techniques used in interpreting LULC change in a study (Rojas 2011).

Table 8: The Year 2015 PCA of the study area

Bands	Minimum	Maximum	Mean	Standard Deviation	Eigen Values
PC1	0.013780	0.020317	0.014558	0.000478	0.000025
PC 2	0.011631	0.019592	0.012552	0.000639	0.000009
PC 3	0.009226	0.020314	0.010804	0.000875	0.000001
PC 4	0.006932	0.024129	0.009045	0.001593	0.000000
PC 5	0.008665	0.042075	0.027242	0.002975	0.000000
PC 6	0.004266	0.046896	0.019923	0.003177	0.000000
PC 7	0.002324	0.051162	0.010936	0.003393	0.000000

PC: Principal component.

Table 9: The year 2020 PCA of the study area

Bands	Minimum	Maximum	Mean	Standard Deviation	Eigen Values
PC 1	0.018748	0.020297	0.019207	0.000210	0.000009
PC 2	0.017424	0.019254	0.017896	0.000271	0.000001
PC 3	0.015415	0.018353	0.016065	0.000411	0.000000
PC 4	0.014264	0.019298	0.015470	0.000721	0.000000
PC 5	0.018575	0.028806	0.024057	0.000836	0.000000

PC 6	0.013239	0.053289	0.022143	0.001866	0.000000
PC 7	0.007797	0.135582	0.013936	0.002293	0.000000

PC: Principal component.

Table 10: The Year 2015 PCA Eigenvector of the study area

Eigenvector	PC 1	PC 2	PC 3	PC 4	PC 5	PC6	PC 7
Band 1	0.084	0.116	0.162	0.309	-0.081	0.623	0.680
Band 2	0.013	0.019	-0.016	0.043	-0.984	-0.172	0.019
Band 3	0.262	0.320	0.405	0.479	0.136	-0.620	0.182
Band 4	0.157	0.198	0.287	0.394	-0.071	0.436	-0.709
Band 5	-0.481	-0.476	-0.257	0.683	0.034	-0.089	-0.022
Band 6	-0.378	-0.381	0.813	-0.224	-0.034	-0.001	0.017
Band 7	0.725	-0.688	0.025	0.041	-0.002	0.000	0.002

PC: Principal component.

Table 11: The year 2020 PCA Eigenvector of the study area

Eigenvector	PC 1	PC 2	PC 3	PC 4	PC 5	PC 6	PC 7
Band 1	-0.055	-0.075	-0.116	-0.218	-0.058	-0.603	-0.751
Band 2	-0.006	0.003	0.047	0.006	0.963	0.159	-0.211
Band 3	-0.156	-0.214	-0.333	-0.420	-0.173	0.703	-0.344
Band 4	0.243	0.283	0.354	0.560	-0.190	0.339	-0.521
Band 5	-0.725	-0.390	-0.109	0.556	-0.007	-0.019	-0.037
Band 6	-0.596	0.429	0.570	-0.363	-0.039	0.037	-0.009
Band 7	0.183	-0.729	0.641	-0.149	-0.033	0.020	-0.011

PC: Principal component.

Land-use changes from 2015 to 2020

The analyzed TCC (True color composite) reveals that there are 5 major types of LULC in the study area namely: bareground, farmland, wetland, vegetation, and built-up areas. The land-use classification maps obtained from the TCC was displayed in Figure 9. The result of the land use classification maps showed that wetland and farmland are the dominant land use classes with total areas of about 60% (Table 12). It was observed from the land use classification map that built-up, wetland, bareground, vegetation and farmland had respective areas of 2.7%, 22.6%, 19.7%, 22.8%, and 32.3% in the year 2015. Consequently, in the year 2020, vegetation decreased from 2277.1 ha to 1098.3ha, and an increase was observed in farmland, wetland, bareground, and built-up areas in the following order: 33.9%, 27.8%, 24.0%, and 3.3% respectively. The increase observed in the wetland in the year 2020 could contribute to regulations of climate change in the study area. Mitsch et al. (2012) opined that an appreciable increase in wetlands serves as a climate change regulator and supports atmospheric carbon-dioxide reduction. The result of the post-classification showed that the area under wetland, bareground, farmland and built-up areas increased in the following order: 517.9ha, 431.8ha, 169.2ha, and 59.9ha, and a decrease was observed in vegetation cover (Table 13). The decreased in vegetation observed may be traced or attributed to an increase in human activities in the study area during the past 5 years.

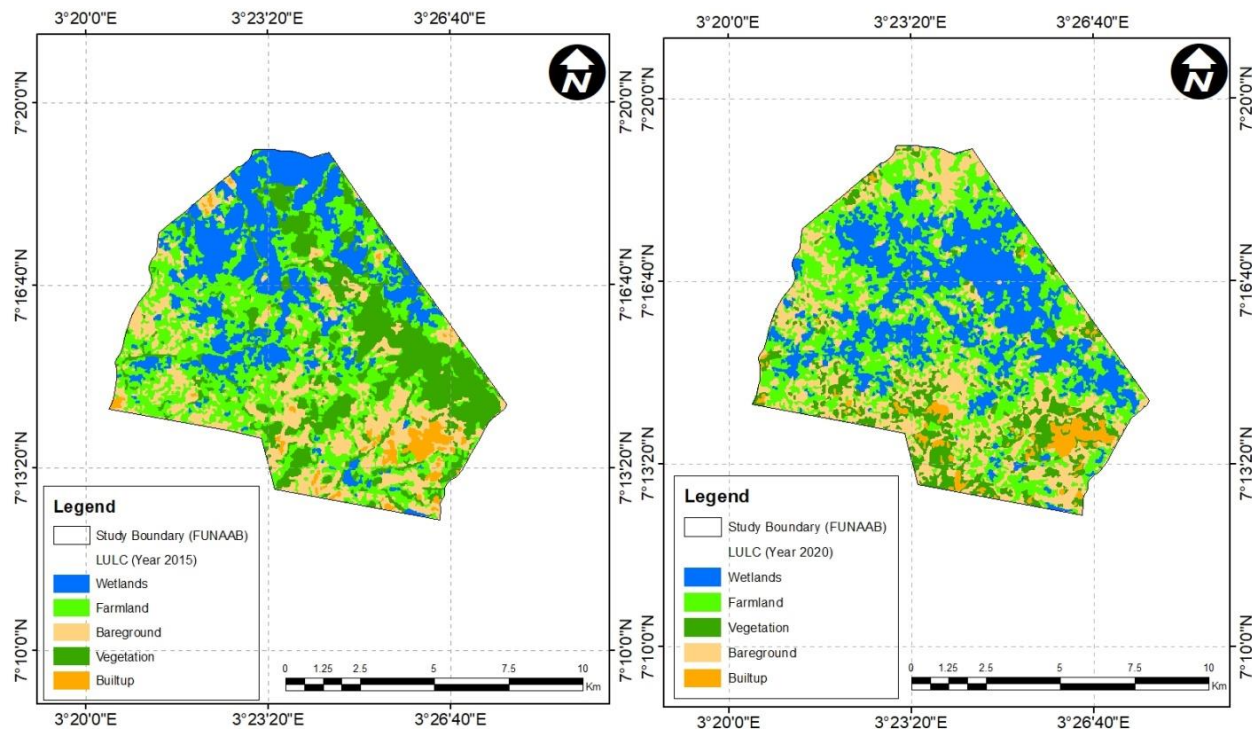


Figure 9: Land use and land cover of the study area

Table 12: Land use and land cover classification of the study area.

LULC class	2015		2020	
	Ha	%	Ha	%
Builtup	266.7	2.7	326.6	3.3
Wetland	2263.3	22.6	2781.2	27.8
Bareground	1972.9	19.7	2404.7	24.0
Vegetation	2277.1	22.8	1098.3	11.0
Farmland	3228.2	32.3	3397.4	33.9
Total	10008.2	100	10008.2	100

Ha: Hectare, %: Percentage

Table 13: Change detection of the study area

LULC class	Area (Ha) in year	Area (Ha) in year	Change detection (Ha) between 2015 and 2020
	2015	2020	
Builtup	266.7	326.6	59.9 (Increase)
Wetland	2263.3	2781.2	517.9 (Increase)
Bareground	1972.9	2404.7	431.8 (Increase)
Vegetation	2277.1	1098.3	1178.8 (Decrease)
Farmland	3228.2	3397.4	169.2 (Increase)

Ha: Hectare

Accuracy Assessment and Analysis

Accuracy assessment is the most important part of remote sensing and land-use change classifications (Li, 2005). The kappa coefficient and overall accuracy were used to verify the accuracy of the land use classification of the study area. In this study, the classification overall accuracy efficiency reached 89.47% and 92.22% respectively. The MLSC algorithm applied in the Landsat 8 satellite images in this study showed that wetland, farmland, vegetation, background, and builtup areas were accurately classified with 83.33% and 88.57% kappa coefficient (Tables 14 and 15).

Table 14: Error matrix and accuracy assessment of the land use map for 2015

Land use	Wetland	Farmland	Builtup	Bareground	Vegetation	Total	Producer Accuracy (%)	User Accuracy (%)
Wetland	40	0	0	10	3	53	93.02	75.47
Farmland	0	72	0	0	3	75	93.51	96.00
Builtup	1	3	31	1	3	39	86.11	79.49
Bareground	2	2	0	60	0	64	84.51	93.75
Vegetation	0	0	5	0	52	57	86.25	91.23
Total	43	77	36	71	61	288		
Overall accuracy = 89.47 % Kappa coefficient=83.33%								

Table 15: Error matrix and accuracy assessment of the land use map for 2020

Land use	Wetland	Farmland	Builtup	Bareground	Vegetation	Total	Producer Accuracy (%)	User Accuracy (%)
Wetland	30	0	2	0	10	42	78.94	71.42
Farmland	7	59	0	5	3	74	85.50	79.72
Builtup	0	0	92	12	0	104	97.87	88.46
Bareground	0	10	0	112	0	122	86.82	91.80
Vegetation	1	0	0	0	300	301	95.84	99.67
Total	38	69	94	129	313	643		
Overall accuracy = 92.22 % Kappa coefficient = 88.57 %								

Descriptive Statistics of the analyzed soil properties

The descriptive statistical summary of the analyzed soil properties was presented in Table (16). The soil pH values were ranging from 5.2 to 8.63 with a mean of 6.71, which was also similar to the median values of 6.61. The concentration of soil Organic matter (OM) ranged from low to high (0.6 to 5.8%), with a mean of 3.22%. Total nitrogen (TN) was relatively low (ranging from 0.29 to 0.03%), with a median of 0.17%, and a mean of 0.16%. Available phosphorus, potassium, and Cation exchanged capacity (CEC) were within their respective medium ranges. The micronutrients measured showed that zinc was very high (range > 1.0 mg kg⁻¹) with a median of 9.4 mg kg⁻¹ and a mean of 10.61 mg kg⁻¹ while copper and magnesium were also very high. For copper, the range was > 0.5 mg kg⁻¹ with a mean of 2.98 mg kg⁻¹ and a median of 2.40 mg kg⁻¹. Magnesium also had a mean of 1.64 mg kg⁻¹ with a median of 1.57 mg kg⁻¹. It was observed that the majority of the soil properties had low skewness with a soil texture ranging from 4.58 to 90.5 % for sand, -0.39 to 12.5% for silt, and 1.88 to 17.0% for clay. ⁹²Kravchenko and Bullock (1999) reported that soil properties with low skewness (<1) yielded the most accurate estimates of soil properties. The present study also interdem with the work done by Pal et al. (2010); Sharma et al. (2011); Wang and Shao (2013) that estimating spatial variability of physical and chemical soil properties serves as one of the prerequisites for soil and crop-specific management techniques.

Table 16: Descriptive statistics for the studied soil properties

Variable	Min	Max	Mean	Median	Skewness	Kurtosis	Standard Deviation
Soil pH	5.20	8.63	6.71	6.61	0.56	1.14	0.71
Organic matter	0.69	5.85	3.22	3.34	0.09	-1.29	1.70
Total Nitrogen	0.29	0.03	0.16	0.17	0.05	-1.26	0.08
Phosphorus	0.15	18.52	2.47	1.41	3.27	10.54	4.18
Potassium	0.06	0.36	0.18	0.18	0.49	0.70	0.06
Zinc	7.00	25.00	10.61	9.4	2.77	7.51	4.25
Magnesium	0.72	2.71	1.64	1.57	0.29	0.05	0.47
Copper	0.90	10.4	2.98	2.40	2.83	9.86	1.88
Sand	74.5	90.5	84.50	86.5	-0.74	-0.44	4.58
Silt	0.5	12.5	6.74	6.5	0.20	-0.39	3.21
Clay	7.00	17.0	8.76	8.00	1.88	4.18	2.45

CEC	3.99	17.37	10.32	9.47	0.61	0.14	3.45
-----	------	-------	-------	------	------	------	------

Min: Minimum; Max: Maximum; CEC: Cation exchanged capacity.

Digital soil mapping using IDW

The variability of soil nutrients across the study area calls for a proper soil management strategy. The spatial distribution map of the selected chemical soil properties was produced by IDW (Inverse distance weighted) techniques and the results were grouped into various classes based on the range representing their magnitude in the studied soil (Figures 10 to 12).

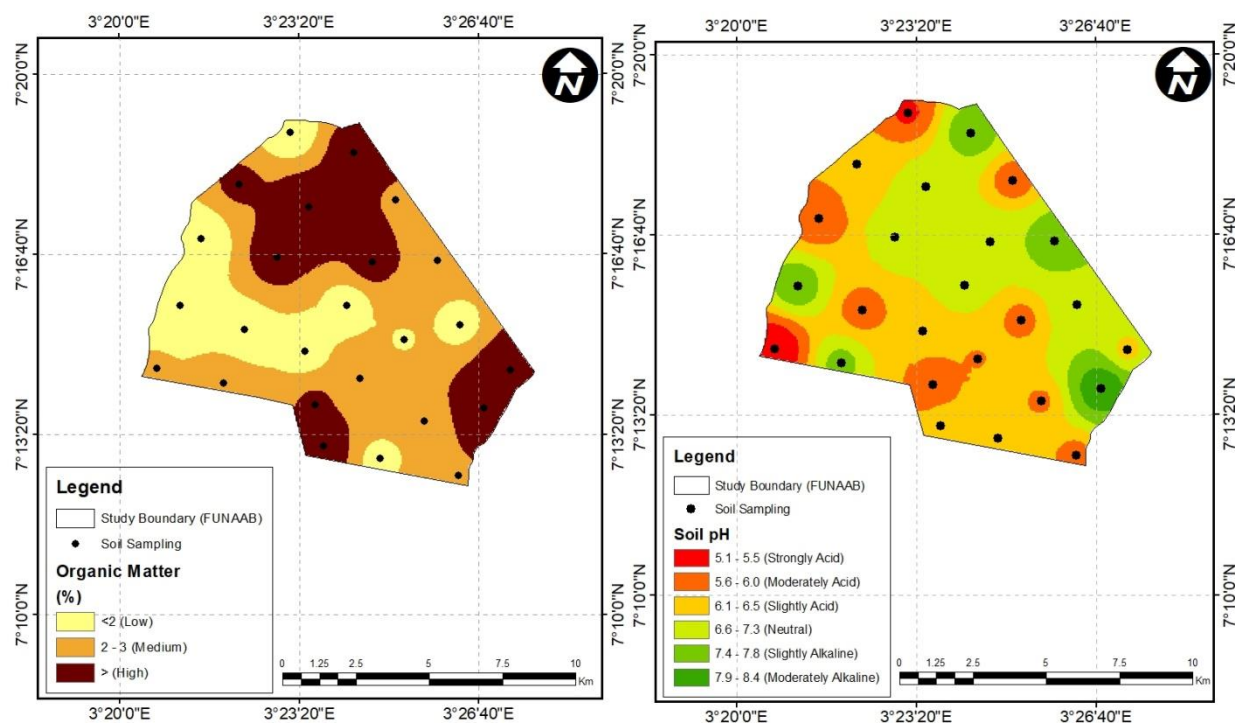


Figure 10: Soil pH and Soil OM

Soil pH varied from strongly acidic (< 5.5) to moderately alkaline (> 8.4) in the study area. These results are in agreement with those reported in a recent study by Tobore et al., (2020). However, the variation in the soil pH observed could be attributed to the nature of the alluvial parent material, micro-topography, and the types of fertilizer used at the time of cultivating the study area⁹⁷ (Vasu et al. 2017). According to Bremner and Mulvaney (1982), Westarp et al. (2004), Regmi and Zebisch (2004) reported that soil management practices such as crop nutrient uptake and harvest without replenishment with poor crop residues management could be responsible for the acidic nature in the present studied soil.

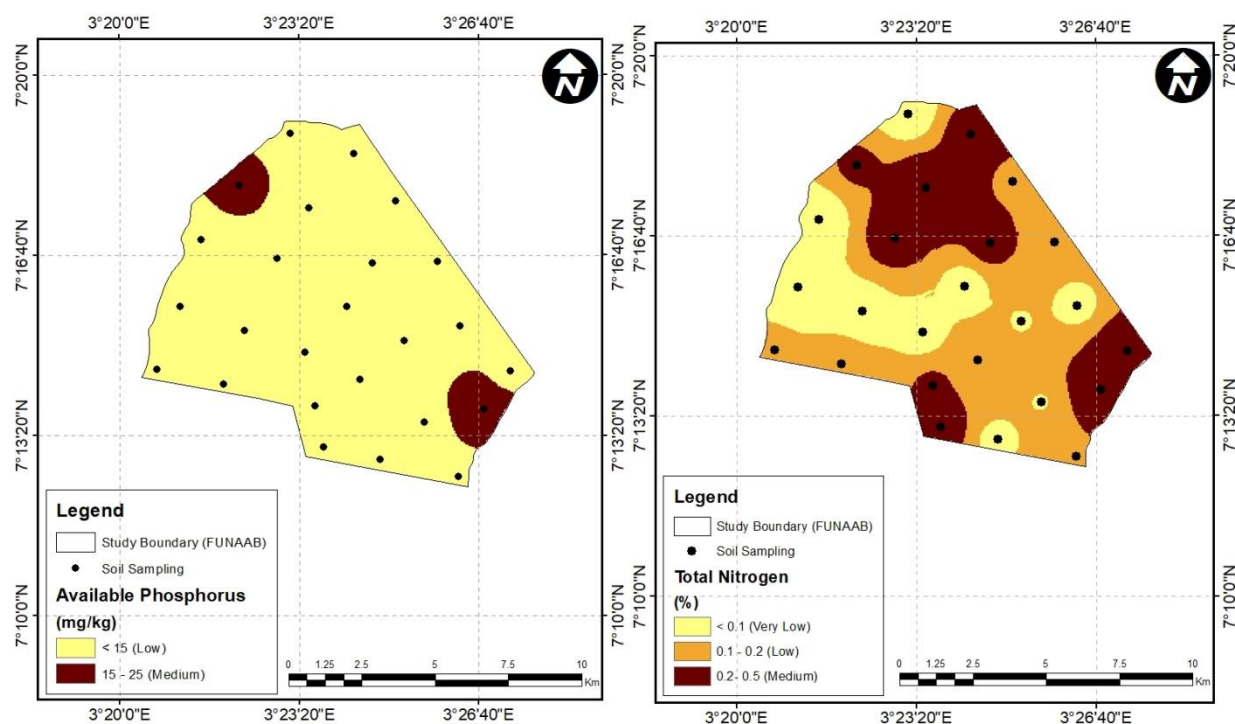


Figure 11: Total N and Available Phosphorus

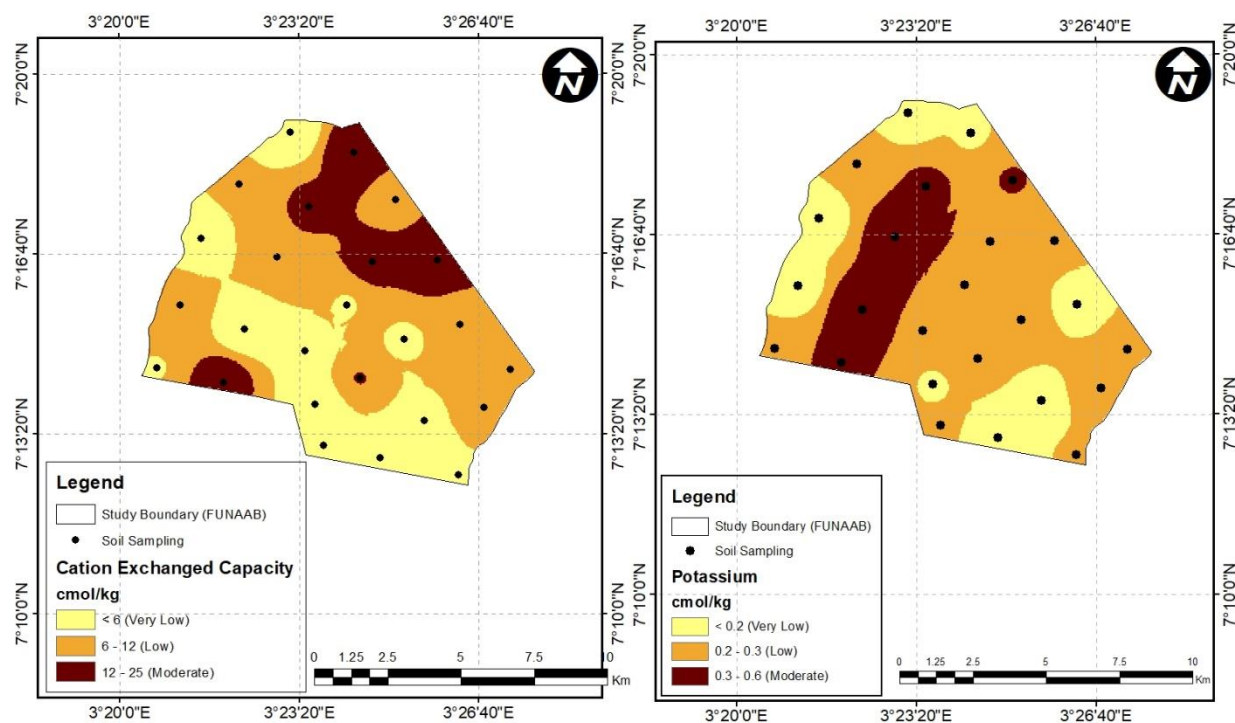


Figure 12: CEC and Potassium

The soil OM (Organic matter) was relatively low (<2%) in the majority of the study area, followed by medium (2 – 3%) and high in > 3%. The low organic matter content in the study soils could be traced to the acidic nature of the soil pH thereby leading to low levels of soil OM in the studied soil. Besides, poor management practices and loss of vegetation could also be responsible for the low soil OM in the studied soil.

Total nitrogen (TN) was deficient in the study area with values < 0.2 % (low and very low) and medium with > 0.2 - 0.5%. The low variation in TN content in the study soil may be related to low soil OM content and the application of inappropriate fertilizer. For instance, the increased rate of mineralization and insufficient application of nitrogen fertilizer to crops such as maize could also be responsible for the low of TN in the studied soil (Sherchan and Gurung, 1995).

The available phosphorus was medium with values > 15 and low with values <15 in the study area. The low soil OM may account for the low level of available phosphorus in the studied soils.

The potassium concentration in the study soil ranged from very low (<0.2cmol/kg), low (0.2 – 0.3cmol/kg) and moderate (0.3 – 0.6 cmol/kg) in the study area. The majority of the CEC was low with values ranging from very low (<6 cmol/kg), low (6 – 12cmol/kg), and medium (12 -25cmol/kg) in the study area. The effect of the low potassium and CEC may be attributed to continuous or yearly cultivation of the study soils for cropping practices.

Determining criteria weights using AHP

The present study employed AHP as a systematic approach to conduct MCDM in the study area. To produce the land suitability map of the study area for rice production, the criteria maps produced were used in line with the result of the AHP in MCDM. The criteria spatial layers of the relative importance were derived and the most important criterion for decision making used in this study was listed in Table (17) based on the pairwise comparison. The common scale of 0 to 100% was obtained from the AHP procedure and the consistency ratio of the pair-wise matrix was 7.5%. This implies that the comparison is less than 10% and thus considered suitable to weighted overlay using each criterion.

Table 17: Resulting weights for the criteria based on pairwise comparison

	LST	MNDWI	LULC	SAVI	EBBI	Soil data	Priority (%)	Rank
LST	1	2	0.5	2	2	2	23	1
MMDWI	0.5	1	1	1	1	0.5	21	2
LULC	2	1	1	1	2	1	20	3
SAVI	0.5	1	1	1	0.5	2	14	4
EBBI	0.5	1	0.5	2	1	1	12	5
Soil data	0.5	1	1	0.5	1	1	10	6

MCDM within GIS

The potential wetland suitability of the study area was generated by integrating the thematic map layers of LST, MNDWI, LULC, SAVI, EBBI, and analyzed soil data in ArcGIS 10 ESRI. The integrated raster layers were classified into three classes namely: marginally not suitable (N1), marginally suitable (S3), and moderately suitable (S2). The classified land suitability map was overlaid with the soil map of the study area. The result of the land suitability map shows that 28.9% of the area was moderately suitable, 33.2% was marginally suitable, and 37.9% was marginally not suitable for rice production (Figure 13). The result of the marginally not suitable (N1) could be traced to anthropogenic activities in the study area. The area with moderately (S2) and marginally (S3) suitable can be used for rice cultivation in the study area. However, there is a need to add appropriate fertilizers (from organic and inorganic sources) to the soil to increase fertility status.

4. CONCLUSION

The importance of wetlands to humankind and the environment requires spatial immediate intervention especially in developing countries such as Nigeria. The main objective of this study was to assess the wetland's potential suitability for rice production using remote sensing data and a GIS-based conceptual framework. The GIS-based conceptual framework combines through AHP has helped to adequately and efficiently map the study area for rice production in less time. The selection of multi-criteria factors used in this study shows that spectral indices (such as LST, LULC, MNDWI, EBBI, and SAVI) and the interpolated soil maps can help to facilitate easy identification of wetlands potentials and assist farmers in identifying the expected nutrient levels in the study area. Besides, the spatial distribution and mapping will aid farmers and various soil users to understand the present conditions of the different land use of the study area. These results can be implemented by the GIS techniques to overcome future threats that may pose to the wetland of the study area.

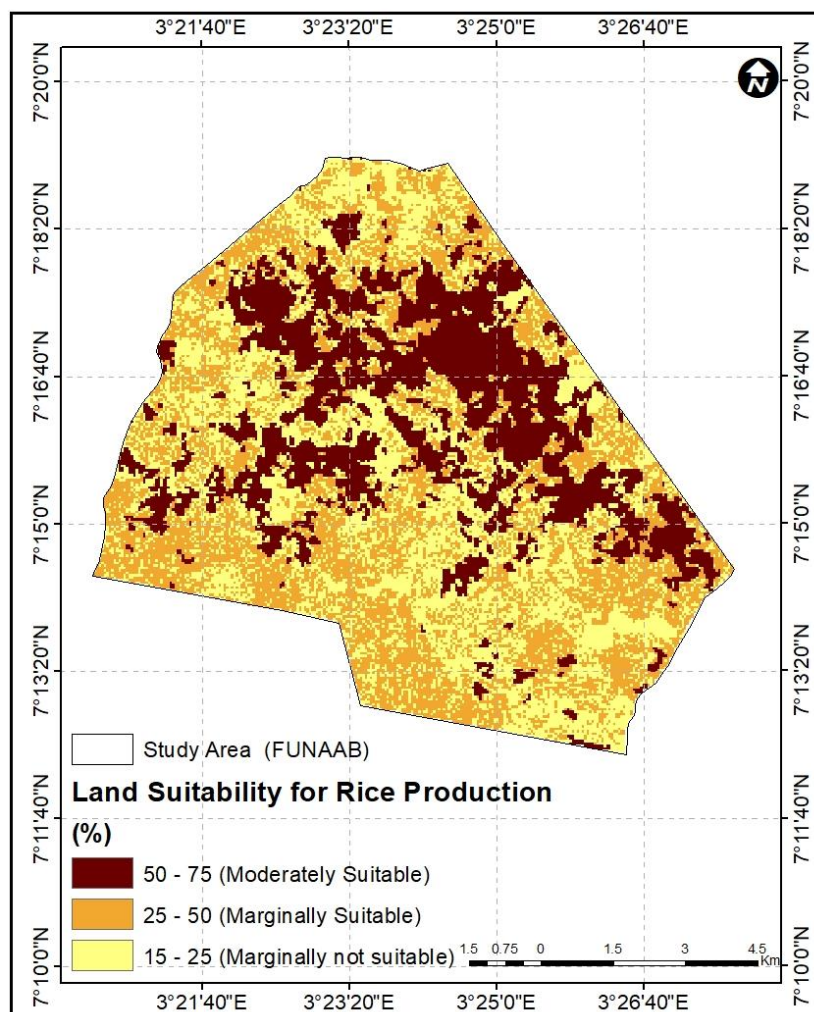


Figure 13: Land suitability for rice production.

Acknowledgment

The authors are sincerely grateful to the Federal University of Agriculture Abeokuta, (FUNAAB) for their understanding and for allowing us to carry out this study. We are equally thankful to the United States Geological Survey (USGS) for assisting this research with data-sets. Tobore Anthony developed the original idea for this research, drafts the methodology, interprets, analyzes the dataset, and finalizes the impact of the wetland on the studied soils. Prof. Senjobi and Dr. Adedeji provide a guideline for writing and Olalere Sodiq made language correction.

Funding:

This study has not received any external funding.

Conflict of Interest:

The authors declare that there are no conflicts of interests.

Peer-review:

External peer-review was done through double-blind method.

Data and materials availability:

All data associated with this study are present in the paper.

REFERENCE

1. Adegoke, C. W., Sojobi, A. O., 2015. Climate change impact on Infrastructure in Osogbo Metropolis, South-west Nigeria. *Journal of Emerging Trends in Engineering and Applied Sciences* 6: 156–165.
2. Ajiboye, G. A., Ogunwale, J. A., 2013. Forms and distribution of potassium in particle size reactions on talc overburden soils in Nigeria. *Archives of Agronomy and Soil Science*, 247–258.
Akisanola, A. A., Ogunjobi, K. O., 2014. Analysis of Rainfall and Temperature Variability over Nigeria. *Global Journal of Human Social Sciences. Geography & Environmental GeoSciences* 14 (3): 1–18.
3. Ayolagha, G. A., Peter, K.D., Ebie, 2012. Effect of remediation of crude oil polluted inceptisols on maize (*Zea mays*) production using organic and inorganic fertilizers at Yenagoa, Bayelsa state.
4. Adebekun, O., 1978. Atlas of the Federal Republic of Nigeria. 1st Edn. Under the Chairmanship of the National Atlas Committee, pp: 136.
5. Anderson, J. R., Hardy, J. T. R., Witmer, R. E., 1976. A land use and land cover classification Agris., 1998. AgLink reference manual. Version 5.3, AGRIS Corp., Rosewell., G. A., pp. 147–171.
6. Ahukaemere, C. M., Akpan, E. L., 2012. Fertility status and characterization of paddy soils of Amasiri in Ebonyi-State, South-eastern Nigeria.;8 (2):159-168.
7. As-syakur, A., Adnyana, I., Arthana, I.W., Nuarsa, I.W., 2012. Enhanced Built-Up and Bareness Index (EBBI) for Mapping Built-Up and Bare Land in an Urban Area. *Remote Sens.* 4, 2957–2970.
8. Bouhennache, R., Bouden, T., Taleb, A.A., Chaddad, A., 2015. Extraction of urban land features from TM Landsat image using the land features index and Tasseled cap transformation. *Recent Advances on Electrosience and Computers*. 2015, pp. 142-147, ISBN: 978-1-61804-290-3
9. Bouyoucos, G.H., 1962. Hydrometer method for making particle size analysis of soils. *Agronomy*. <https://doi.org/10.2134/agronj1962.00021962005400050028x>.
10. Biro, K., Pradhan, B., Buchroithner, M., Makeschin, F., 2013. Land use/Land cover change analysis and its impact on soil properties in the northern part of Gadarif region, Sudan, *Land Degrad. Dev.* 24, 90–102, <https://doi.org/10.1002/ldr.1116>.
11. Bremner, D. C., Mulvaney, J. M., 1982. Total nitrogen in *Methods of Soil Analysis*. (eds Page AL, Miller RH. Keaney DR). American Society of Agronomy. 9 (2).
12. Chuvieco, E., Huete, A., 2002. *Fundamentals of satellite remote sensing*. Boca Raton (FL): Taylor & Francis.
13. Chavez, P. S., 1998. An improved dark-object subtraction technique for atmospheric scattering correction for multispectral data. *Remote Sens Environ.* 24:459–479.
14. Cengiz, T., Akbulak, C., 2009. Application of analytical hierarchy process and geographic information systems in land-use suitability evaluation: a case study of Dumrek village (Çanakkale, Turkey). *Int J Sustain Develop World Ecology* 16 (4):286–294.
15. Congalton, R.G., 1991. A Review of Assessing the Accuracy of Classifications of Remotely Sensed Data. *Remote Sensing of Environment*, 37, 35–46.
16. Chowdary, J.S., Xie, S.P., Luo, J.J., Hafner, J., Behera, S., Masumoto, Y., Yamagata, T., 2010. Predictability of Northwest pacific climate during summer and the role of the tropical Indian Ocean, *Clim.Dyn.*, doi: 10.1007/s00382-009-0686-5.
17. d'Entremont, R.P., Thomason, L.W., 1987. Interpreting meteorological satellite images using a color-composite technique. *Bull. Am. Meteorol. Soc.* 68 (7), 762–768.
18. Ekanade, O., 2007. *Cultured Trees, their Environment and our Legacies*. Inaugural Lecture Series University Press Ltd., Obafemi Awolowo, pp: 44.
Estornell, J., MarGavila, M., Sebastia, MT., Mengual, J., 2013. Principal component analysis applied to remote sensing. *MSEL*. 6:83–89.
19. FAO, 1976. A framework for land evaluation. FAO soil bulletin no.32, Rome.
20. FAO/IUSS Working Group, 2006. A framework for land evaluation. Rome: *Soils Bulletin* 31, pp 564 25-42.
21. FAO., 2007a. Land Evaluation, towards a revised framework. FAO, Rome, Italy.
22. Foody, G.M., 2002. Status of land cover classification accuracy assessment. *Remote Sens. Environ.* 80 (1), 185–201.
23. Fasina, A.S., 2005. Properties and classification of some selected Wetland soils in Ado Ekiti, Southwest Nigeria. *Applied Tropical Agriculture*, 10 (2): 76-82.
24. Frenken, K., Mharapara, I., 2002. Wetland Development and Management in SADC Countries", *Proceedings of a sub-regional workshop held by FAO sub-regional office for East and Southern Africa (SAFR)*, Harare, Zimbabwe, November 19-23, 2001.
25. Gilabert, M.A., Gonzalez, J.P., Melia, J., 2002. A generalized soil-adjusted vegetation index. *Remote Sensing of Environment* 82, p (304).
26. Gilbert, D.A.E., 1969. *A Map Book of West Africa Metric Edition*. Macmillan Education Ltd., London and Basingstoke, pp: 66.
27. Good, T., Giordano, P.A., 2019. Methods for Constructing a Color Composite Image.
28. Huete, A. R., 1988. A soil-adjusted vegetation index. *Remote Sensing of Environment*, 25 (3), 295–309.
29. Harvey, K.R., Hill, G.J.E., 2001. Vegetation mapping of a tropical freshwater swamp in the Northern Territory, Australia: a comparison of aerial photography, Landsat TM

- and SPOT satellite imagery. *Int J Remote Sensing* 22, 2911-2925.
30. Jiang, Z., Huete, A. R., Chen, J., Chen, Y., Li, J., Yan, G., 2006. Analysis of NDVI and scaled difference vegetation index retrievals of vegetation fraction. *Remote Sensing of Environment*, 101 (3), 366–378. <https://doi.org/10.1016/j.rsenv.2006.01.003>.
 31. Jesus, J. B., Santana, I. D. M., 2017. Estimation of land surface temperature in coating area using Landsat8 data, 150–157.
 32. Joshua, J.K., Anyanwu, N.C., Ahmed, A.J., 2013. Land suitability analysis for agricultural planning using GIS and multi criteria decision analysis approach in Greater Kuru Urban Area, Nasarawa State, Nigeria. *Afr J Agric Sci Technol* 1 (1):14–23.
 33. Kravchenko, A. N., Bullock, D. G., 1999. A comparative study of interpolation methods for mapping soil properties. *Agronomy Journal* 91 (3): 393–400.
 34. Koutsias, N., Mallinis, G., Karteris, M., 2009. A Forward Backward Principal Component Analysis of Landsat-7 ETM Data to Enhance the Spectral Signal of Burnt Surfaces," *ISPRS Journal of Photogrammetry and Remote Sensing*, Vol. 64, No. 1, 2009, pp. 37–46. doi:10.1016/j.isprsjprs.2008.06.004.
 35. Kahinda, J. M., Lillie, E. S. B., Taigbenu, A. E., Taute, M., Boroto, R. J., 2008. Developing Suitability Maps for Rainwater Harvesting in South Africa." *Physics and Chemistry of the Earth, Parts A/B/C* 33 (8–13): 788–799. doi:10.1016/j.pce.2008.06.047.
 - Karimi, H., Zeinivand, H., 2019. Integrating Runoff Map of a Spatially Distributed Model and Thematic Layers for Identifying Potential Rainwater Harvesting Suitability Sites Using GIS Techniques. *Geocarto International* 1–20. doi:10.1080/10106049.2019.1608590.
 36. Li, H., Wang, C., Zhong, C., Su, A., Xiong, C., Wang, J., Liu, J., 2017. Mapping Urban Bare Land Automatically from Landsat Imagery with a Simple Index. *Remote Sensing*.
 37. Liu, H., 2005. Accuracy analysis of remote sensing change detection by rule-based rationality evaluation with post-classification comparison. *International Journal of Remote Sensing*, 25 (5), 1037–1050. 483 <http://dx.doi.org/10.1080/0143116031000150004>.
 38. Li, B., Chen, D., Wu, S., Zhou, S., Wang, T., Chen, H., 2016. Spatio-temporal assessment of urbanization impacts on ecosystem services: Case study of Nanjing City China- *Ecological Indicators* 71; 416–427.
 39. Mitsch, W.J., Gosselink, J.G., 1993. *Wetlands*. Second edition. New York: Van Nostrand Reinhold.
 40. McLean, E. O., Dumford, S. W. F., Coronel, S. W., 1982. A comparison of several methods of determining lime requirements of soil. *Soil Science Society of America Proceedings* 30 -26.
 - Mitsch W.J., Bernal B, Nahlik A.M, 2012. Wetlands, carbon, and climate change *Landscape Ecol* DOI 10.1007/s10980-012-9758-8.
 41. McCartney M., Rebelo, L.M., Senaratna, S.S., de Silva, S., 2010. *Wetlands Agriculture and Poverty Reduction*. Colombo, Sri. Lanka: International Water Management Institute. IWMI Research Report. 39p.
 42. Mahmoud, S. H., Alazba, A. A., 2014. The Potential of in Situ Rainwater Harvesting in Arid Regions: Developing a Methodology to Identify Suitable Areas Using GIS-based Decision Support System." *Arabian Journal of Geosciences* 8: 1–13.
 43. McFeeters, S.K., 1996. The use of Normalized difference water index (NDWI) in the delineation of open water features. *International Journal of Remote Sensing*. 17: 1425–1432.
 44. Mustafa, A. A., Singh, M., Sahoo, R. N., Ahmed, N., Khanna, M., Sarangi, A., Mishra, A. K., 2011. Land suitability analysis for different crops: a multi criteria decision making approach using remote sensing and GIS. *Researcher*.3: 1–84.
 45. MA, 2005b. *Ecosystems and human Well-being: Wetlands and water Synthesis*. World Resources Institute, Washington, DC.
 46. Nelson, D. W., Sommers, L. E., 1996. Total carbon, organic carbon, and organic matter. In D.L. Sparke (Ed.), *Methods of soil analysis*. Part3. Chemical methods SSSA book series no. 5 (pp. 961–1010). Madison: ASA and SSSA.
 47. Sinha, P., Verma, N.K., Ayele, E., 2016. Urban Built-up Area Extraction and Change Detection of Adama Municipal Area using Time-Series Landsat Images. *International Journal of Advanced Remote Sensing and GIS*. 2016, 5 (8), pp. 1886–1895.
 48. Ojanuga, A. G., 2006. *Agro-ecological zones of Nigeria manual*. FAO/NSPFS, Federal Ministry of Agriculture and Rural Development, Abuja, Nigeria.;124.
 - Patil, V.D, Sankhua, R.N., Jain, R.K., 2012. Analytic hierarchy process for evaluation of environmental factors for residential land use suitability. *Int J Comput Eng Res* 2 (7):182–189.
 49. Pal, S., Panwar, P., Bhatt, V.K., 2010. Analysis and interpretation of spatial variability of soil properties is a keystone in site-specific management. *Indian Journal of Soil Conservation* 38 (3): 178–183.
 50. Pontius Jr, R.G., Millones, M., 2011. Death to Kappa: birth of quantity disagreement and allocation disagreement for accuracy assessment. *Int. J. Rem. Sens.* 32 (15), 4407–4429.
 51. Regmi, B. D., Zebisch, M. A., 2004. Soil fertility status of Bari and Khet land in a small watershed of middle hill region of Nepal. *Nepal Agricultural Research Journal*; 5:38–44.
 52. Rojas, S., 2011. Assessment of a methodology for satellite image processing for change use land identification. Thesis presented to obtain the degree of Geographer and

- Environment EngineerSangolq Army Polytechnic School. Spanish.
53. Rasul, A., Balzter, H., Smith, C., 2015. Spatial Variation of the Daytime Surface Urban Cool Island during the Dry Season in Erbil, Iraqi Kurdistan, from Landsat 8. *Urban Climate* 14: 176–186. doi:10.1016/j.uclim.2015.09.001.
 54. Sun, Y., Zhou, Q., Xie, X., Liu, R., 2013. Spatial, sources and risk assessment of heavy metal contamination of urban soils in typical regions of Shenyang, China. *Journal of Hazardous Materials*. 174 (1–3), 455–462 <https://doi.org/10.1016/j.jhazmat.2009.09.074>.
 55. Soil survey staff, 2010. Key to soil taxonomy,. Washington D. C.: USDA soil conservation service revised edition (9th).
 56. Sotona, T., Salako, F., Adesodun, J., 2014. Soil physical properties of selected soil series in relation to compaction and erosion on farmers' fields at Abeokuta, southwestern Nigeria, *Archives of Agronomy and Soil Science*, 60:6, 841–857, DOI: 10.1080/03650340.2013.844334.
 57. Sharma, P., Shukla, K., Mexal, G., 2011. Spatial variability of soil properties in agricultural fields of southern New Mexico. *Soil Science* 176 (6): 288–302.
 58. Singh, A., Harrison, A., 2005. Standardized Principal Components," *International Journal of Remote Sensing*, Vol. 6, No. 6, , pp. 883–896. doi:10.1080/01431168508948511.
 59. Sys, I., Van Ranst, E., Debaveye, J., 1991. Land evaluation, Part I. Principles in land evaluation and crop production calculations, General administration for development cooperation, Brussels, p.40.
 - Saaty, T.L., 1980. The analytical hierarchy process. McGraw Hill, NewYork.
 60. Smyth, A. J.,Montgomery, R. F., 1962. Soils and Land Use in Central Western Nigeria. Govt. Printer, Ibadan, Western Nigeria: 264pp.
 61. Sys, I., Van Ranst, E., Debaveye, J., 1991. Land evaluation, part I. Principles in land evaluation and crop production calculations," General administration for development cooperation, Brussels, pp. 40–80.
 62. Saaty, T. L., 2001. Fundamentals of the analytic hierarchy process. In: Schmoldt DL, Kangas J, Mendoza, G. A., and Pesonen, M., (eds) The analytic hierarchy process in natural resource and environmental decision making. Kluwer Academic Publishers, Netherlands, pp 15–35. ISBN 0-7923-7076-7.
 63. Saaty, T. L., 1977. A scaling method for priorities in hierarchical structures, *J Math Psychol*, 681 vol. 15, pp. 234–281. 1977.
 64. Thapa, R. B., Murayama, Y., 2007a. Image classification techniques in mapping urban landscape: a case study of Tsukuba city using AVNIR-2 sensor data. *Tsukuba GeoenviromSci* 3:3–10.
 65. Thapa, R. B., Murayama, Y., 2008b. Land evaluation for peri-urban agriculture using analytical hierarchical process and geographic information system techniques: a case study of Hanoi. *Land Use Policy* 25 (2):225–239.
 66. Ufoegbune, G.C., Oyedepo, J.A., Awomeso, A., Eruola, O., 2010. Spatial Analysis of Municipal Water Supply in Abeokuta Metropolis, South Western Nigeria. REAL CORP Proceedings. Tagungsband: Vienna, Austria. 18– 20 May 2010. <http://www.corp.at>. M. Schrenk, V. Vasily, P. Popovich, and P. Zeile (eds.).
 67. Vasu, D., Singh, S.K., Sahu, N., Tiwary, P., Chandran, P., Duraisami, V.P., 2017. Assessment of spatial variability of soil properties using geospatial techniques for farm level nutrient management. *Soil and Tillage Research*. 169:25–34.
 - Vargahan, B., Shahbazi, F., Hajrasouli, M., 2011. Quantitative And Qualitative Land Suitability Evaluation For Maize Cultivation In Ghobadlou Region, Iran, *Ozean Journal of Applied Sciences*, vol. 4, no. 1, Issn 1943–2429.
 68. Verbesselt, J., Somers, B., Van, Aardt., J., Jonckheere, I., Coppin, P., 2006b. Monitoring herbaceous biomass and water content with SPOT VEGETATION time-series to improve fire risk assessment in savanna ecosystems, *Remote Sensing of Environment*, 101, 3, 399–414.
 69. Walkley, A., Black, I. A., 1934. An examination of the Degtjareff method for determining soil organic matter and proposed modification of the chromic acid titration method. *Soil Science* 37:29 – 38.
 70. Weng, Q., 2012. An introduction to contemporary remote sensing. New York: The McGraw-Hill Companies.
 71. Wang, Y. Q., Shao, M. A., 2013. Spatial variability of soil physical properties in a region of the loess plateau of PR China subject to wind and water erosion. *Land Degradation and Development* 24 (3): 296–304.
 72. Wang, N., Ma, Q., Ding, H., Liang, H., 2018. Detection of urban expansion and land surface temperature change using multi-temporal Landsat images-Resources Conservation and Recycling 128: 526–534.
 73. Westarp, S.V., Sandra, Brown, H.S., Shah, P.B., 2004. Agricultural intensification and the impacts on soil fertility in the Middle Mountains of Nepal. *Canadian journal of soil science*. Aug 1; 84 (3):323–32.
 74. Xu, H., (2005): A Study on Information Extraction of Water Body with the Modified Normalized Difference Water Index (MNDWI). *Journal of Remote Sensing*. 9: 589–595.
 75. Yang, D., Robinson, D., Zhao, Y., Estilow, T., Ye, B., 2003. Streamflow response to seasonal snow cover extent changes in large Siberian watersheds, *Journal of Geophysics Research*, vol. 108, pp. 4578.
 76. Zhang, J., Niu, J., Bao, T., Buyantuyev, A., Zhang, Q., Dong, J., Zhang, X., 2015. Human induced dryland degradation in Ordosplateau, China, revealed by multi-level statistical

modelling of normalized difference vegetation index and rainfall time series, J. Arid Land, 6, 219–229, <https://doi.org/10.1007/s40333-013-0203-x>.